

Supporting Information

A tetraphenylethene-based hexacationic molecular cage with an open cavity

Fan Cao, Honghong Duan, Qingfang Li, and Liping Cao*

College of Chemistry and Materials Science, Northwest University, Xi'an, 710069, P. R. China.

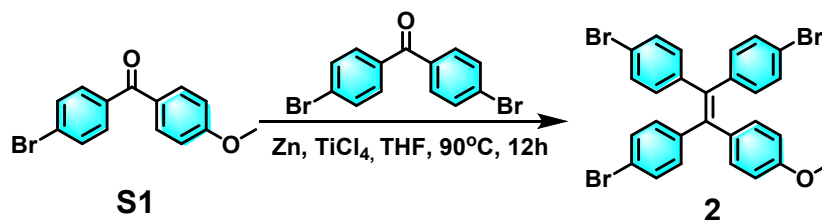
*E-mail: chcaoliping@nwu.edu.cn

Table of Contents	Pages
General experimental details	S2
Synthetic procedures and characterization data	S2
X-ray structure determination	S14
Host-guest chemistry between 1 •6PF ₆ ⁻ and PAHs	S20
Host-guest chemistry between 1 •6Cl ⁻ and dinucleotide molecules	S31

Experimental Procedures

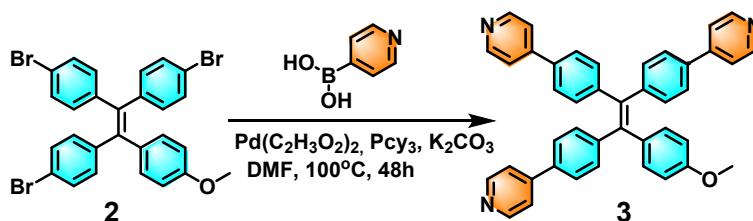
General Experimental Details. Starting materials were purchased from commercial suppliers were used without further purification. Melting points were recorded by using a WRS-1A apparatus in open capillary tubes. IR spectra were measured on a TENSOR27 spectrometer. NMR spectra were recorded on a spectrometer operating at 400 MHz for ^1H and 100 MHz for ^{13}C NMR spectra on Bruker ascend spectrometer and JEOL spectrometer. Electrospray Ionization (ESI) mass spectra were acquired with Bruker micrOTOF-Q II electrospray instrument. UV/vis spectra were done on Agilent Cary-100 spectrometer. Fluorescence spectra were performed by using a Horiba Fluorolog-3 spectrometer. CD spectra were performed by using JASCO J-1500. Isothermal titration calorimetry (ITC) was carried out using a VP-ITC (Malvern) at 25 °C.

Synthetic Procedures and Characterization Data.

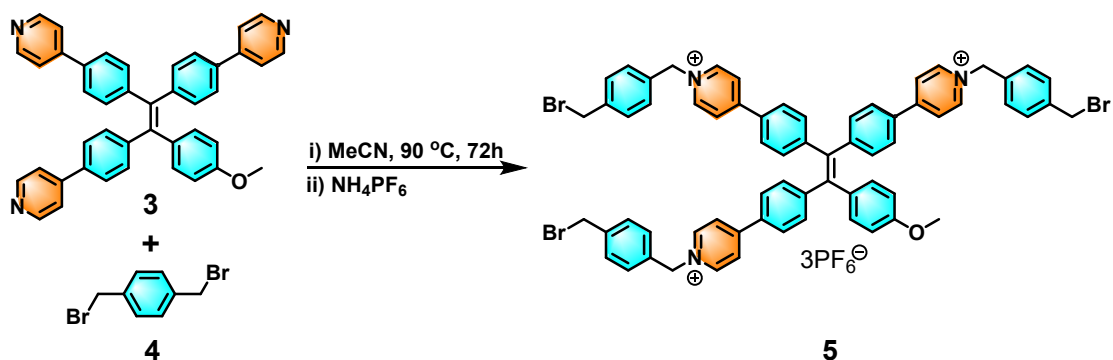


Compound 2. S1 (2.00 g, 6.87 mmol), 4,4'-Dibromobenzophenone (2.57 g, 7.56 mmol) and zinc powder (4.49 g, 68.7 mmol) were added to a 250 mL three-necked flask. Nitrogen was pumped for three times and anhydrous tetrahydrofuran (80 mL) was added at 0°C and stirred for 30 minutes. Titanium tetrachloride (3.8 mL, 34.4 mmol) was added to the reaction small amount for several times, and then heated to 90°C and refluxed for 12 h. The reaction was quenched by adding 10% K₂CO₃ solution. The mixture was extracted by ethyl acetate, washed by saturated NaCl solution, and dried by anhydrous Na₂SO₄. Compound 2 as white powder was obtained by silica gel chromatography with petroleum ether. M.p (1.30 g, yield: 31.5%). > 300 °C. IR (KBr, cm⁻¹): 3440s, 1640s, 1600m, 1246w, 557m. ^1H NMR (400 MHz, CDCl₃): 7.30-7.20 (m,

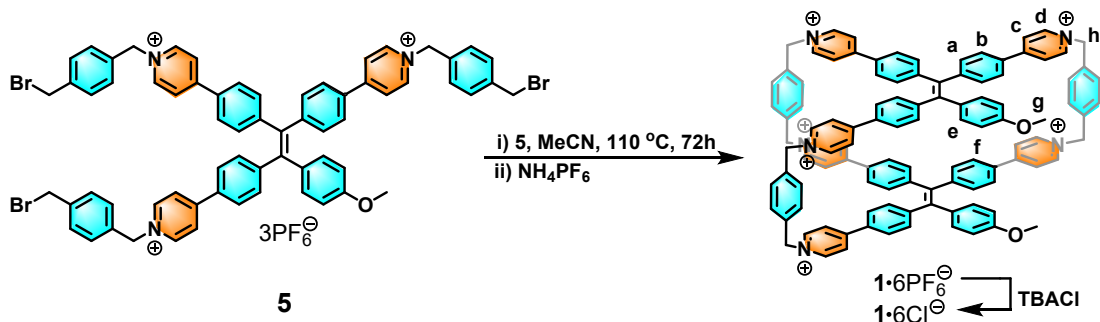
6H), 6.95-6.80 (m, 8H), 6.66 (d, $J = 8.0$, 2H), 3.76 (s, 3H). ^{13}C NMR (101 MHz, CDCl_3): 158.8, 142.4, 142.2, 135.0, 133.1, 132.6, 131.4, 131.3, 121.1, 121.0, 120.9, 113.6, 55.3 (only 13 of the 19 resonances expected were observed due to the similar chemical environment for three bromide benzene rings). ESI-TOF-MS: m/z 597.9037 (calcd. for $[\text{C}_{27}\text{H}_{19}\text{Br}_3\text{O}]$, 597.9025).



Compound 3. **2** (500 mg, 0.83 mmol), 4-pyridine boric acid (615 mg, 5.0 mmol), anhydrous potassium carbonate (692 mg, 5.0 mmol), palladium acetate (186 mg, 0.83 mmol), tricyclohexylphosphine (236 mg, 0.83 mmol) was added into a 100 mL Shrek tube, anhydrous N-N'-dimethylformamide (38 mL) was added in N_2 environment, and heated to 100°C and stirred for 48 h, Then the mixture was cooled to room temperature. **3** as yellow powder was obtained by silica gel chromatography with $V_{\text{DCM}} : V_{\text{MeOH}} = 40 : 1$. (300 mg, yield: 60.6%). M.p. $> 300^\circ\text{C}$. IR (KBr, cm^{-1}): 3440s, 1593s, 1508m, 1398w, 1246m, 1036w, 808s. ^1H NMR (400 MHz, CDCl_3): 8.65-8.55 (m, 6H), 7.55-7.35 (m, 12H), 7.19 (d, $J = 8.0$, 6H), 7.01 (d, $J = 12$, 2H), 6.70 (d, $J = 8.0$, 2H), 3.76 (s, 3H). ^{13}C NMR (101 MHz, CDCl_3): 158.7, 150.4, 147.7, 147.7, 147.7, 144.8, 144.7, 144.7, 141.4, 139.2, 136.3, 136.1, 136.0, 135.4, 132.7, 132.3, 126.5, 126.5, 126.5, 121.4, 113.5, 55.3 (only 21 of the 28 resonances expected were observed due to the similar chemical environment for three pyridyl benzene rings). ESI-TOF-MS: m/z 594.2628 (calcd. for $[\text{C}_{42}\text{H}_{31}\text{N}_3\text{O}]$, 594.2494).



Compound 5. 4 (534 mg, 2.0 mmol) and anhydrous acetonitrile (50 mL) were added to a 250 mL double-necked flask and heated to 90°C for reflux for 30 min. **3** (100 mg, 168 μmol) was dispersed in 5 mL anhydrous acetonitrile, a small amount was added to the reaction several times, and reflux was performed for 72 h. Then the mixture was cooled to room temperature, and the precipitate was collected and washed with an excess amount of acetone (3×25 mL) by centrifuge to give crude product with Br⁻ counterions as orange solid. Crude product with excess amount of NH_4PF_6 in H_2O (20 mL) was dissolved and stirred for 12 h. The precipitate was collected and washed with an excess amount of H_2O (3×20 mL) to give **5** as orange solid (140 mg, yield: 52.8%). M.p. > 300 °C. IR (KBr, cm^{-1}): 3440s, 1637s, 1600m, 1498w, 1246w, 1161w, 841s, 557m. ^1H NMR (400 MHz, CD_3CN): 8.75-8.60 (m, 6H), 8.25-8.10 (m, 6H), 7.85-7.65 (m, 6H), 7.55-7.45 (m, 6H), 7.45-7.35 (m, 6H), 7.35-7.25 (m, 6H), 7.01 (d, $J = 8.3$, 2H), 6.74 (d, $J = 8.3$, 2H), 5.65 (s, 6H), 4.60 (s, 6H), 3.72 (s, 3H). ^{13}C NMR (101 MHz, CD_3CN): 160.1, 156.8, 156.7, 149.1, 148.4, 148.1, 145.2, 145.1, 144.9, 143.8, 140.9, 140.1, 135.6, 135.2, 134.2, 133.3, 133.3, 133.0, 132.8, 131.0, 130.8, 130.4, 129.9, 128.8, 128.6, 128.4, 125.9, 125.8, 114.4, 64.7, 64.0, 55.8, 33.5. (only 33 of the 46 resonances expected were observed due to the similar chemical environment for three pyridinium benzene rings). ESI-TOF-MS: m/z 645.5828 ($[\mathbf{5} \cdot 3\text{PF}_6^- - 2\text{PF}_6^-]^{2+}$, calcd. for $[\text{C}_{66}\text{H}_{55}\text{Br}_3\text{N}_3\text{OP}_2\text{F}_{12}]^{2+}$, 645.5737); 382.0728 ($[\mathbf{5} \cdot 3\text{PF}_6^- - 2\text{PF}_6^-]^{3+}$, calcd. for $[\text{C}_{66}\text{H}_{55}\text{Br}_3\text{N}_3\text{OPF}_6]^{3+}$, 382.0708).



Compound 1·6PF₆⁻. **5** (100 mg, 63 μmol) and anhydrous acetonitrile (100 mL) were added in a 350 mL pressure flask, heated to 90 °C and tetrabutylammonium iodide (4.67 mg, 13 μmol) was added for reflux for 10 min. **3** (45 mg, 76 μmol) was dispersed in anhydrous acetonitrile (4 mL), and suspension of **3** was added into the reaction for several times. The reaction was heated to 110 °C for 72 h. Then the mixture was cooled to room temperature, the orange suspension was centrifuged, and the supernatant was steamed to obtain orange solid crude product with Br⁻ counterions. After being dissolved in water, added excess amount of NH₄PF₆ and stirred for 12h. The precipitate was collected and washed with an excess amount of H₂O (3 × 20 mL) to give crude product with PF₆⁻ counterions as orange solid. The crude product was purified by silica gel chromatography with CH₂Cl₂ : MeCN (saturated NH₄PF₆) = 4:1 (v:v) as mobile phase (6.5 mg, yield: 4.3%). M.p. > 300 °C. IR (KBr, cm⁻¹): 3440s, 1637s, 1600m, 1497w, 1464w, 1246w, 1161w, 559m. ¹H NMR (400 MHz, CD₃CN): 8.75-8.55 (m, 12H), 8.15-7.95 (m, 12H), 7.70-7.45 (m, 24H), 7.22 (d, *J* = 8.0, 4H), 7.18 (d, *J* = 8.0, 4H), 7.14 (d, *J* = 8.0, 4H), 7.00 (d, *J* = 8.0, 4H), 6.77 (d, *J* = 8.0, 4H), 5.75-5.60 (m, 12H), 3.76 (s, 6H). ¹³C NMR (101 MHz, CD₃CN): 160.4, 157.07, 156.8, 156.7, 148.6, 148.2, 148.1, 144.9, 144.8, 144.2, 140.0, 136.6, 136.5, 136.3, 135.4, 133.9, 133.7, 133.6, 133.3, 132.8, 131.6, 131.3, 131.1, 128.7, 126.3, 126.2, 126.1, 114.5, 64.3, 64.2, 55.9 (only 31 of the 37 resonances expected were observed due to the similar chemical environment for six pyridinium benzene rings). ESI-TOF-MS: *m/z* 644.8713 ([**1**·6PF₆⁻ - 3PF₆⁻]³⁺, calcd. for [C₁₀₈H₈₆N₆O₂P₃F₁₈]³⁺, 644.8577); 447.4080 ([**1**·6PF₆⁻ - 4PF₆⁻]⁴⁺, calcd. for [C₁₀₈H₈₆N₆O₂P₂F₁₂]⁴⁺, 447.4018); 328.9330 ([**1**·6PF₆⁻ - 5PF₆⁻]⁵⁺, calcd. for [C₁₀₈H₈₆N₆O₂PF₆]⁵⁺, 328.9287).

Compound 1·6Cl⁻. The solution of **1**·6PF₆⁻ (10 mg, 3.5 μmol) in MeCN (3 mL)

was added excess amount of tetrabutylammonium chloride hydrate (9.7 mg, 35 μmol), and the mixture was stirred for another 12 h. The precipitate was collected and washed with an excess amount of MeCN ($3 \times 5 \text{ mL}$) to give $\mathbf{1} \cdot 6\text{Cl}^-$ as orange solid (5.2 mg, yield: 75.4%). M.p. $> 300 \text{ }^\circ\text{C}$. IR (KBr, cm^{-1}): 3416s, 1635s, 1599m, 1496m, 1462w, 1244w, 1161m, 798m. ^1H NMR (400 MHz, CD_3OD): 9.10-8.90 (m, 12H), 8.30-8.15 (m, 12H), 7.80-7.65 (m, 24H), 7.25 (d, $J = 8.0$, 8H), 7.20 (d, $J = 8.0$, 4H), 7.00 (d, $J = 10$, 4H), 6.74 (d, $J = 10$, 4H), 5.95-5.70 (m, 12H), 3.75 (s, 6H). ^{13}C NMR (101 MHz, CD_3OD): 161.1, 157.6, 157.6, 157.3, 148.2, 148.8, 148.8, 145.6, 145.4, 145.4, 144.8, 140.6, 134.3, 134.3, 134.2, 134.1, 133.9, 133.8, 133.5, 132.0, 131.8, 131.6, 129.2, 129.1, 126.6, 126.4, 126.0, 126.0, 114.8, 64.4, 55.7 (only 31 of the 37 resonances expected were observed due to the similar chemical environment for six pyridinium benzene rings). ESI-TOF-MS: m/z 820.2899 ($[\mathbf{1} \cdot 6\text{Cl}^- - 2\text{Cl}^-]^{2+}$, calcd. for $[\text{C}_{108}\text{H}_{86}\text{N}_6\text{O}_2\text{Cl}_4]^{2+}$, 820.2758); 535.2065 ($[\mathbf{1} \cdot 6\text{Cl}^- - 3\text{Cl}^-]^{3+}$, calcd. for $[\text{C}_{108}\text{H}_{86}\text{N}_6\text{O}_2\text{Cl}_3]^{3+}$, 535.2046); 392.6523 ($[\mathbf{1} \cdot 6\text{Cl}^- - 4\text{Cl}^-]^{4+}$, calcd. for $[\text{C}_{108}\text{H}_{86}\text{N}_6\text{O}_2\text{Cl}_2]^{4+}$, 392.6530); 306.9277 ($[\mathbf{1} \cdot 6\text{Cl}^- - 5\text{Cl}^-]^{5+}$, calcd. for $[\text{C}_{108}\text{H}_{86}\text{N}_6\text{O}_2\text{Cl}]^{5+}$, 306.9297).

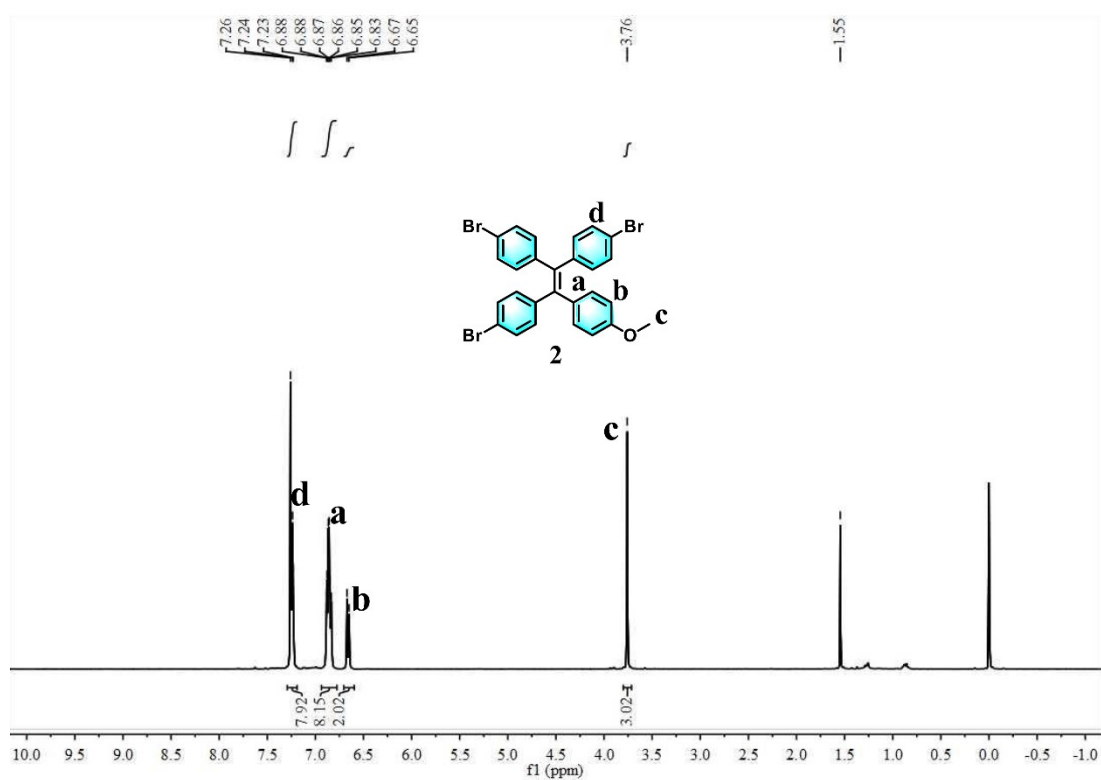


Figure S1. ¹H NMR spectrum recorded (400 MHz, CDCl₃, RT) for **2**.

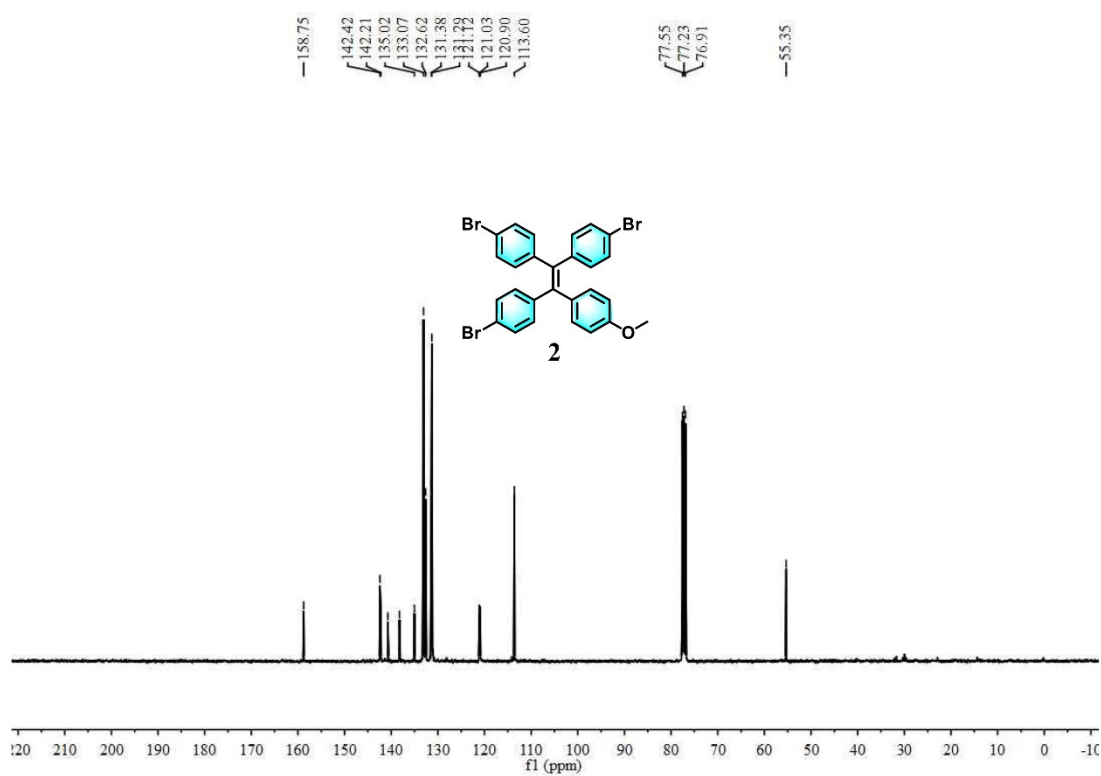


Figure S2. ¹³C NMR spectrum recorded (101 MHz, CDCl₃, RT) for **2**.

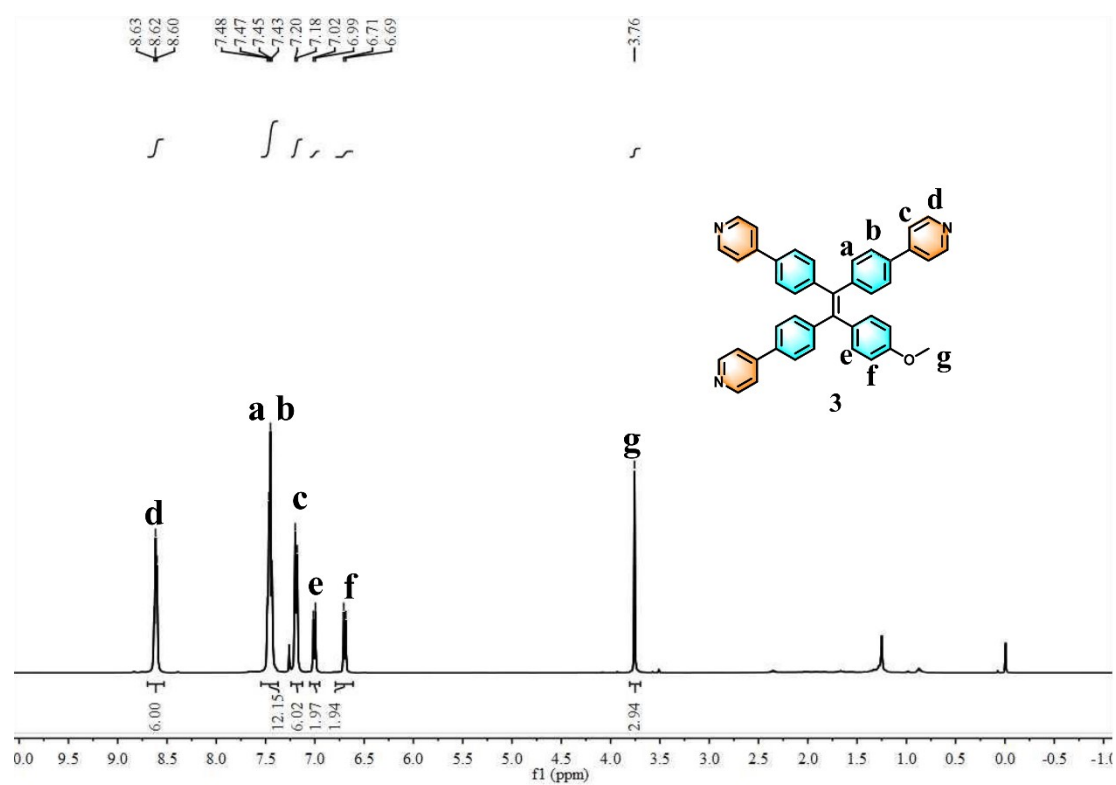


Figure S3. ^1H NMR spectrum recorded (400 MHz, CDCl_3 , RT) for **3**.

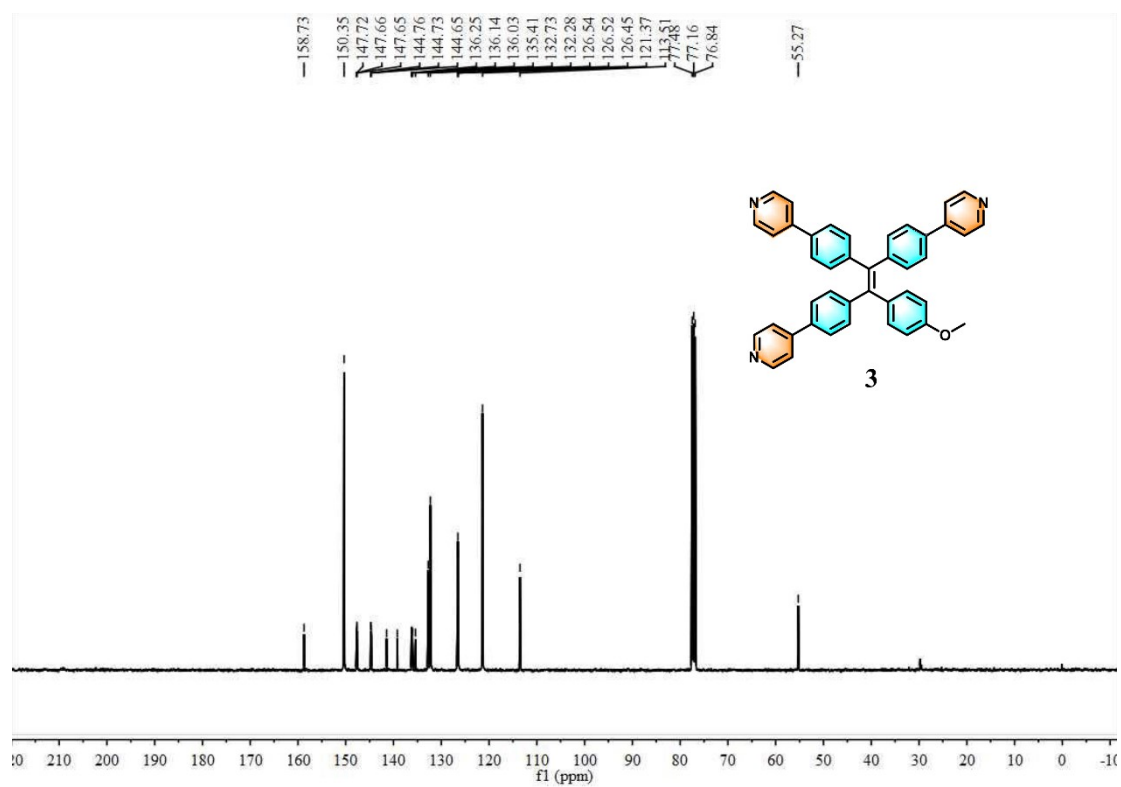


Figure S4. ^{13}C NMR spectrum recorded (101 MHz, CDCl_3 , RT) for **3**.

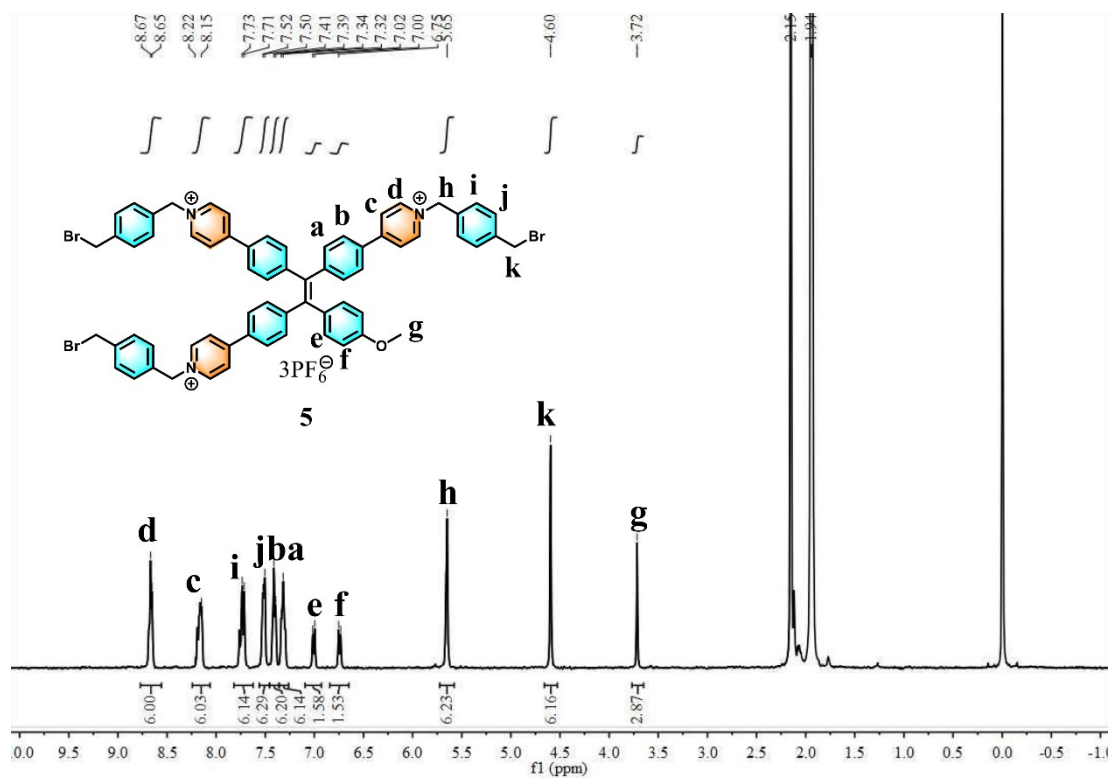


Figure S5. ¹H NMR spectrum recorded (400 MHz, CD₃CN, RT) for **5**.

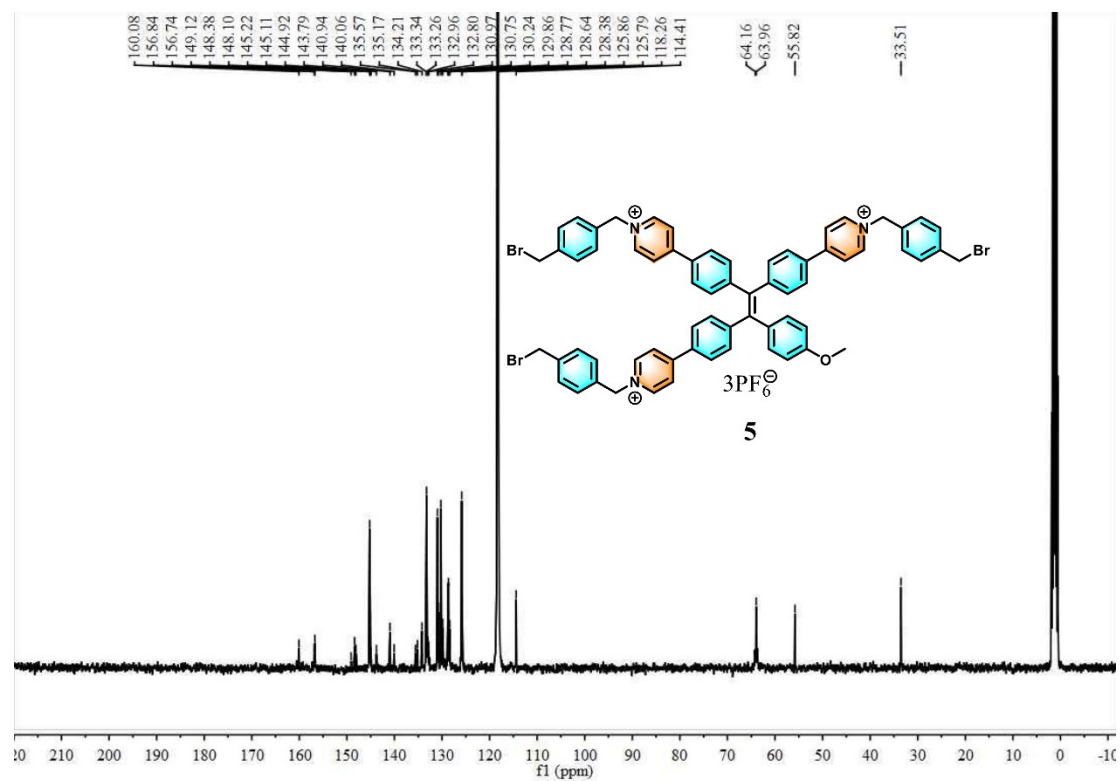


Figure S6. ¹³C NMR spectrum recorded (101 MHz, CD₃CN, RT) for **5**.

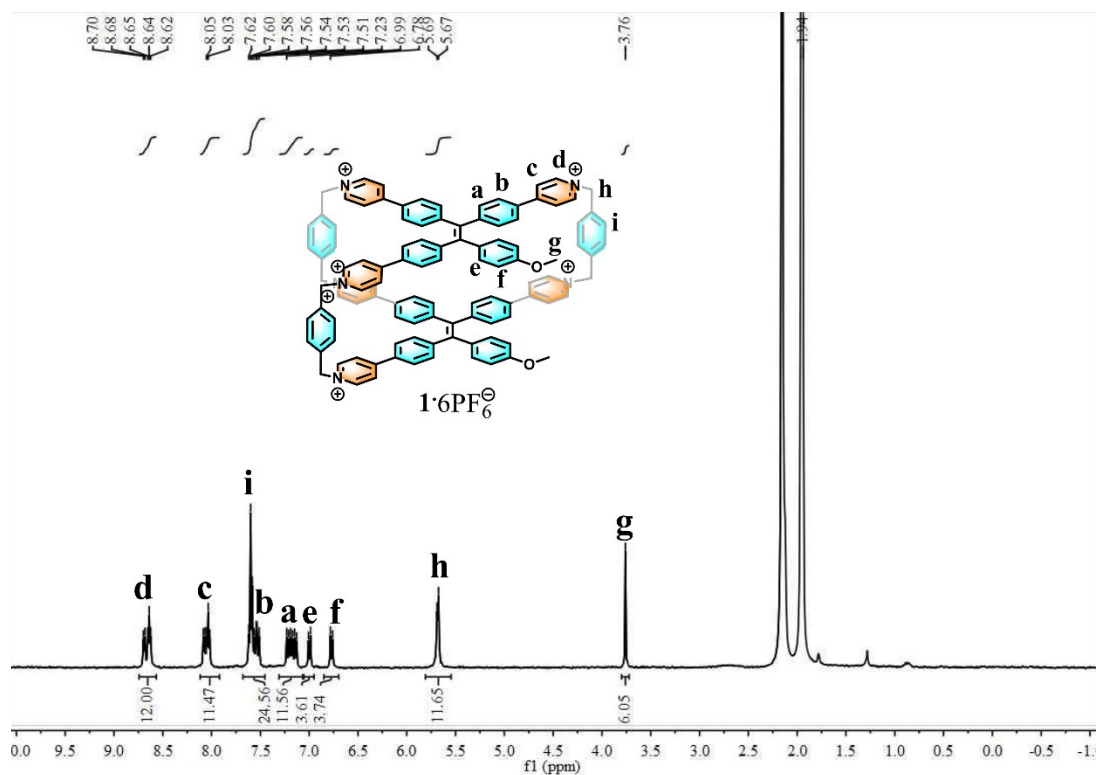


Figure S7. ¹H NMR spectrum recorded (400 MHz, CD₃CN, RT) for **1•6PF₆⁻**.

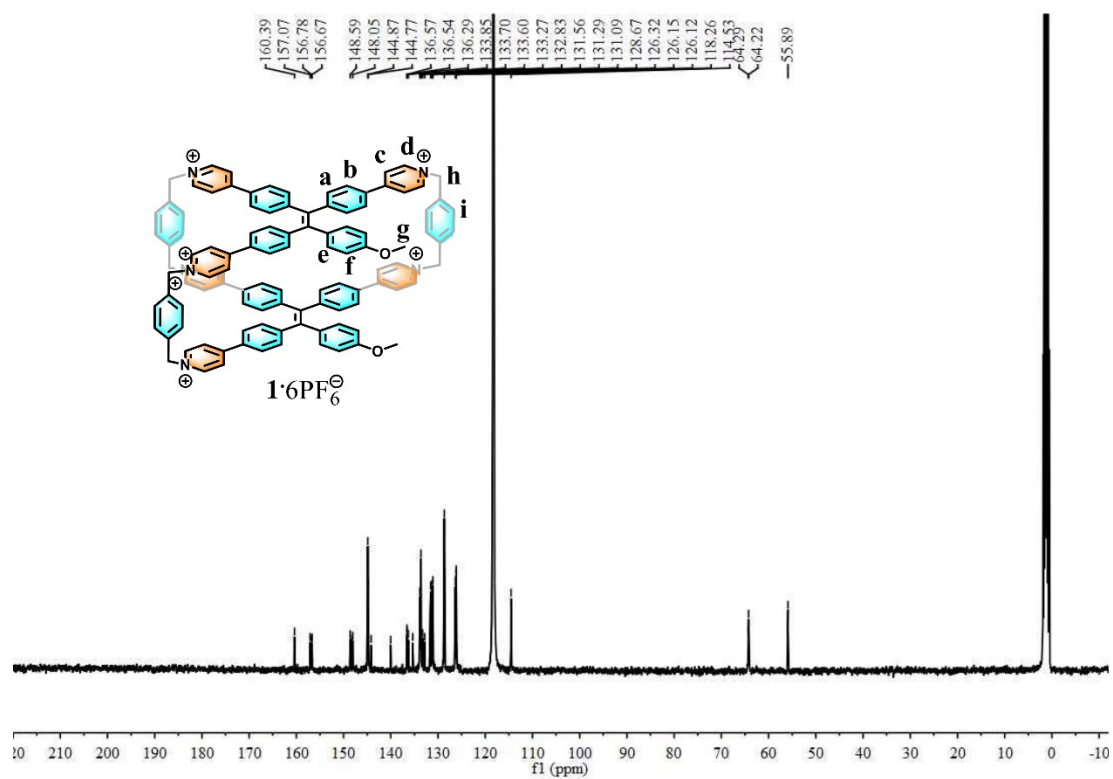


Figure S8. ¹³C NMR spectrum recorded (101 MHz, CD₃CN, RT) for **1•6PF₆⁻**.

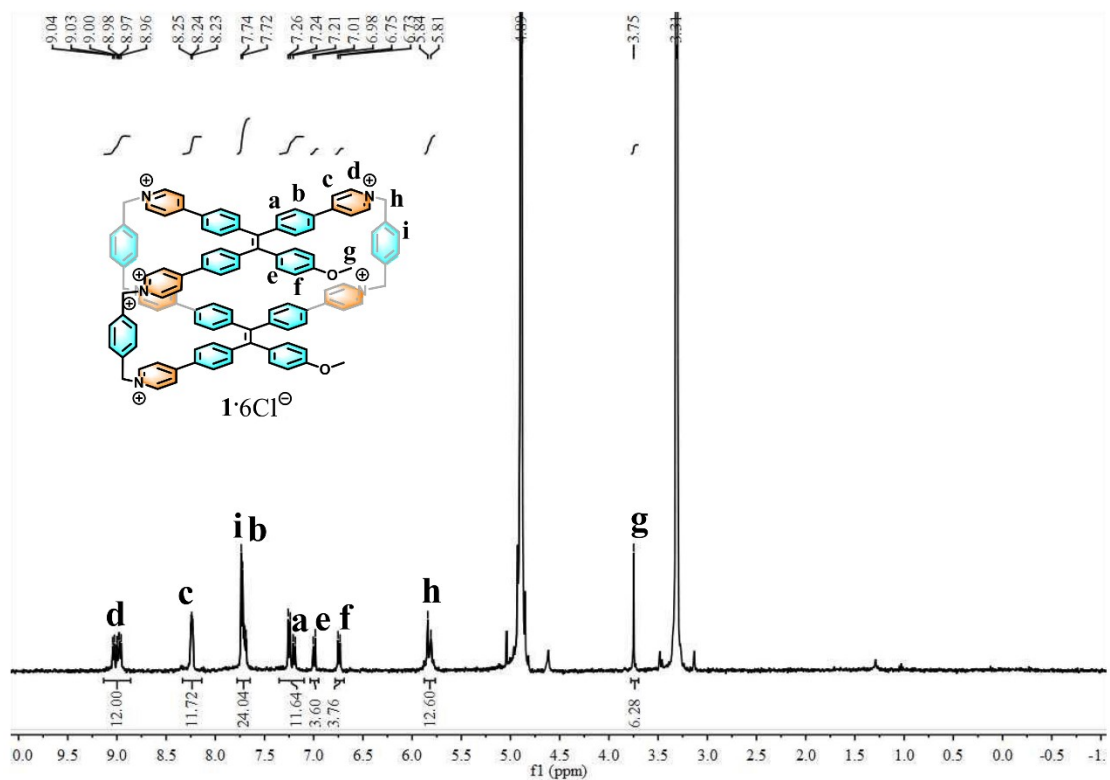


Figure S9. 1H NMR spectrum recorded (400 MHz, CD_3OD , RT) for $1 \cdot 6Cl^-$.

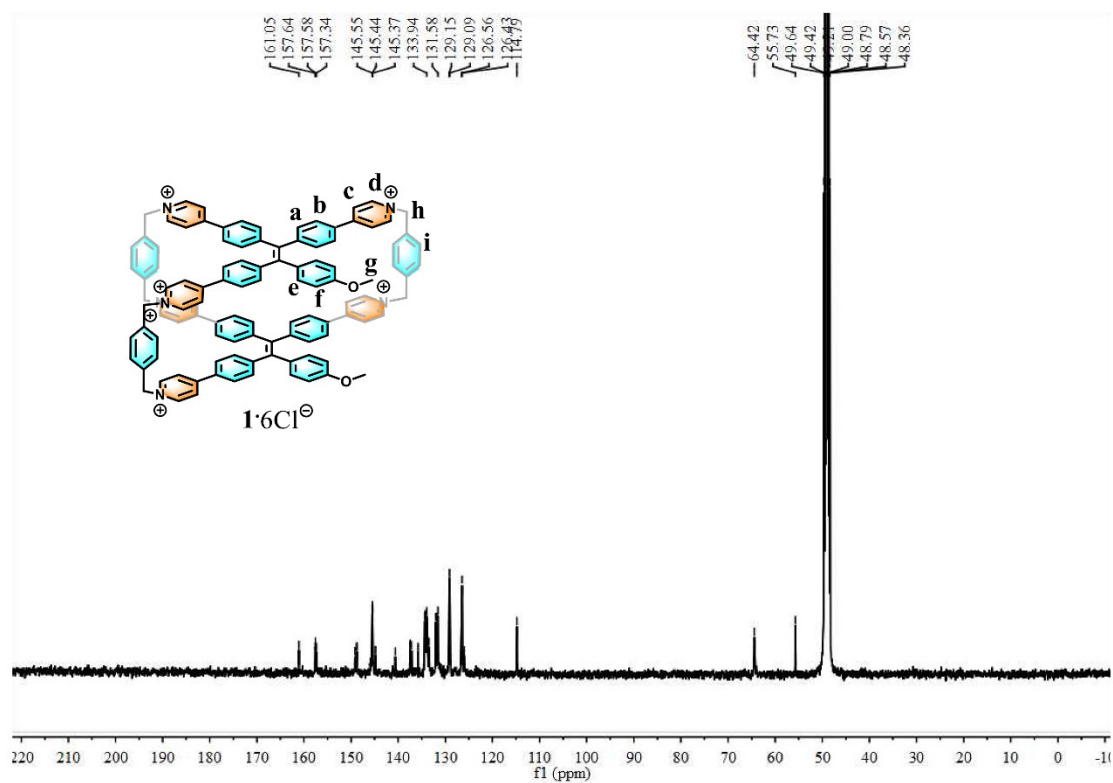


Figure S10. ^{13}C NMR spectrum recorded (101 MHz, CD_3OD , RT) for $1 \cdot 6Cl^-$.

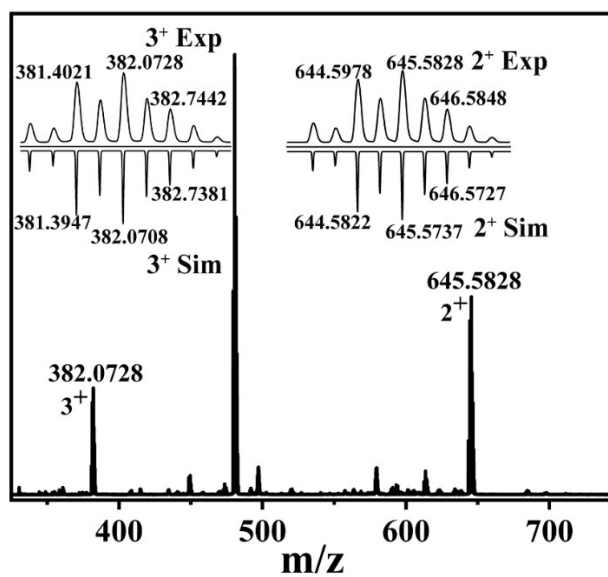


Figure S11. Experimental and calculated electrospray ionization mass spectra of 5.

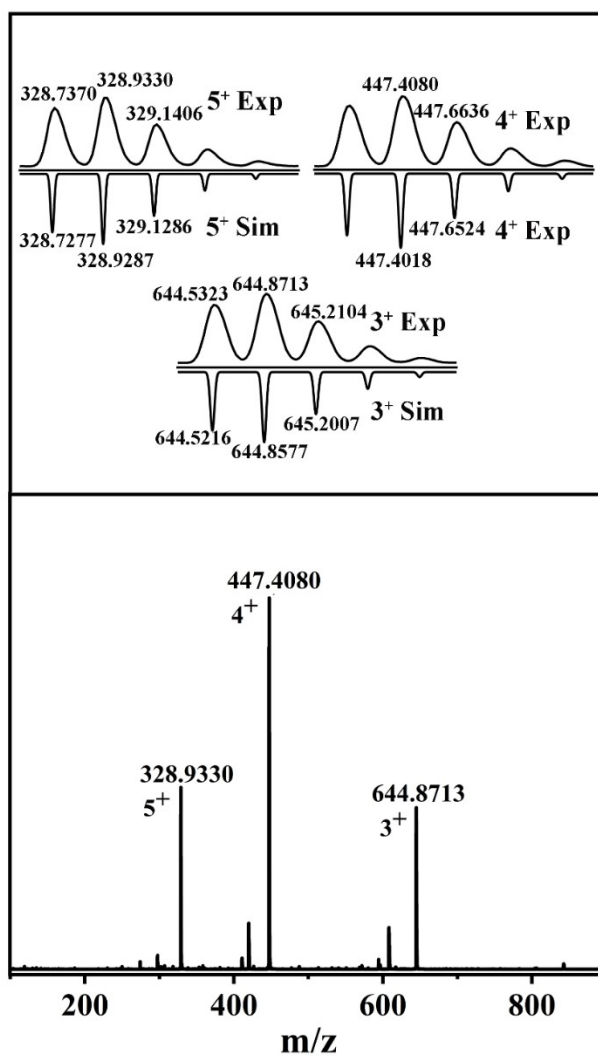


Figure S12. Experimental and calculated electrospray ionization mass spectra of $1 \cdot 6PF_6^-$.

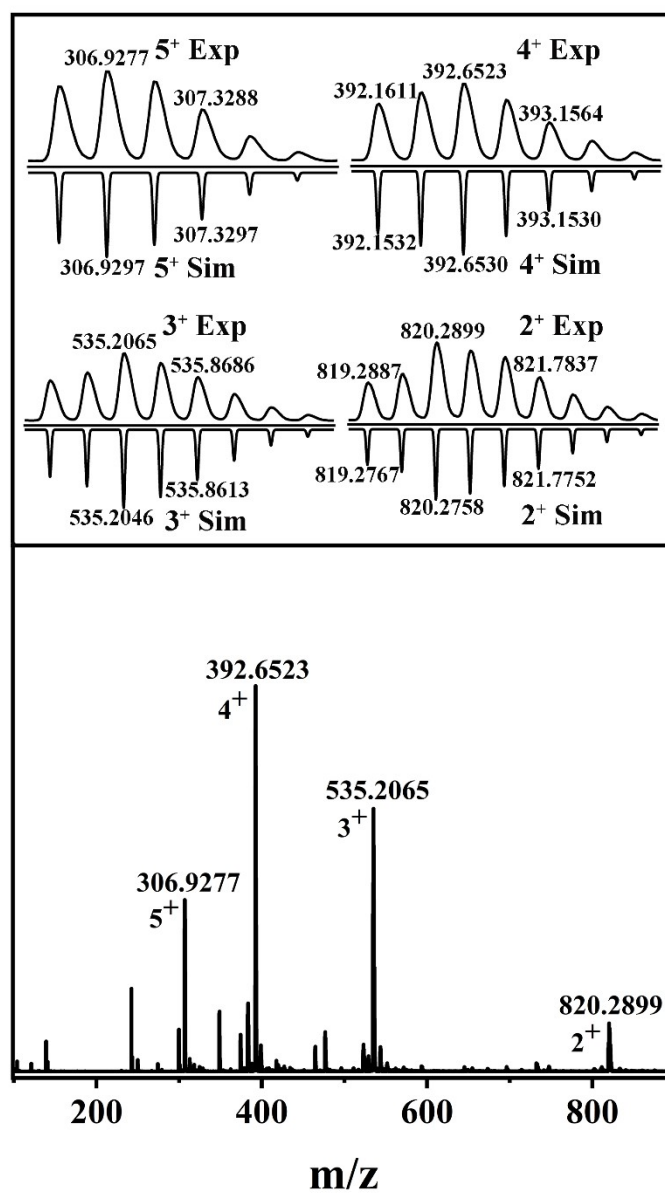


Figure S13. Experimental and calculated electrospray ionization mass spectra of $1 \cdot 6Cl^-$.

X-ray Structure determination.

The crystal of **1**•6Cl⁻: Data collections was performed on Bruker VENTURE system with PHOTON 100 CMOS detector equipped and a Ga-target Liquid METALJET D2 PLUS X-ray Source ($\lambda = 1.34139 \text{ \AA}$). The data was collected at 180 K crystal temperature (Oxford Cryosystems CRYOSTREAM 700), 50 kV and 30 mA with an appropriate $0.5^\circ \omega$ and φ scan strategy. Data reduction and integration were performed with SAINT (version 8.38A). Data was corrected for absorption effects using the empirical methods as implemented in SADABS (version 2016/2). The structure was solved by SHELXT (version 2018/2) and refined by full-matrix least-squares procedures using the SHELXL program (version 2018/3) through the OLEX2 graphical interface. All non-hydrogen atoms, including those in disordered parts, were refined anisotropically. All H-atoms were included at calculated positions and refined as riders, with $U_{iso}(H) = 1.2 U_{eq}(C)$. In each unit cell, there are 70 CH₃OH molecules that were found to be severely disordered and removed by the SQUEEZE routine in PLATON (version 220719).

1•6Cl⁻ was dissolved in CH₃OH and the solution was passed through a 0.10 μm filter into a 10 mL tube, which was placed inside a 500 mL wild-mouth bottle containing isopropyl ether (50 mL). The bottle was capped, after slow evaporation of isopropyl ether at room temperature into the CH₃OH solution for 15 days, and orange single crystals of **1**•6Cl⁻ were obtained

Table S1. Crystal data and structure refinement for **1•6Cl⁻**.

Chemical formula	C ₁₀₈ H ₈₆ Cl ₆ N ₆ O ₂
M _r	1712.52
Temperature	293(2) K
Wavelength	1.34139 Å
Crystal system, Space group	Monoclinic, P 2/n
a, b, c (Å)	32.948(3), 20.5987(16), 41.700(3)
α, β, γ (°)	90, 113.007(4), 90
V(Å ³)	26048(4)
Z	2
Density (calculated)	1.184 Mg/m ³
Absorption coefficient	1.138 mm ⁻¹
F(000)	9884
Crystal size(mm ³)	0.23 x 0.22 x 0.2
Theta range for data collection	1.898 to 52.982°
Index ranges	-39<=h<=39, -24<=k<=24, -46<=l<=49
Reflections collected	234734
Independent reflections	44462 [R(int) = 0.1004]
Completeness to theta = 25.242°	96.5 %
Absorption correction	Semi-empirical from equivalents
Max. and min. transmission	0.9508 and 0.5374
Refinement method	Full-matrix least-squares on F ²
Data / restraints / parameters	44461 / 2372 / 2259
Goodness-of-fit on F ²	1.106
Final R indices [I>2σ(I)]	R ₁ = 0.1197, wR ₂ = 0.2526
R indices (all data)	R ₁ = 0.1758, wR ₂ = 0.2776
Extinction coefficient	n/a
Largest diff. peak and hole	1.331 and -1.275 e.Å ⁻³

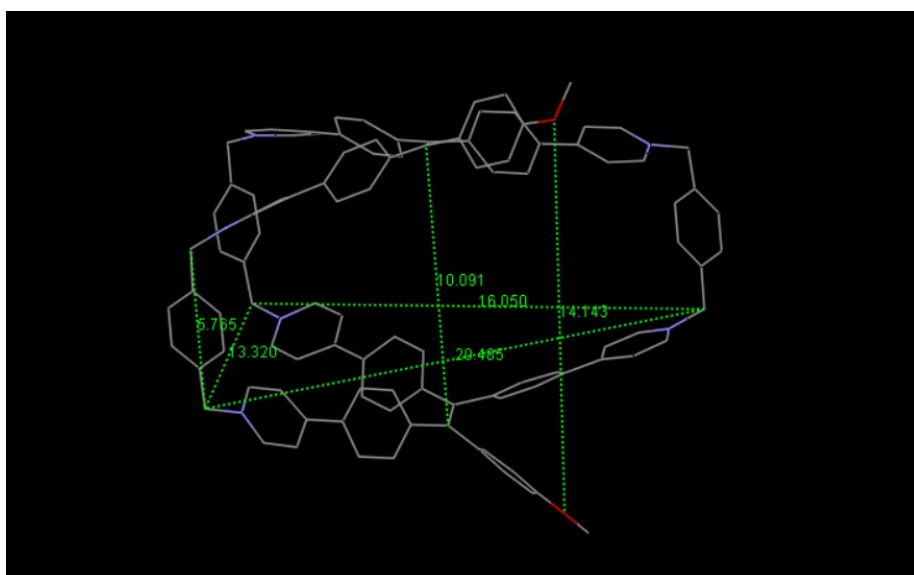


Figure S14. The X-ray structures of **1**•6Cl⁻. Color code: N, blue; C, gray; H, white; O, red.

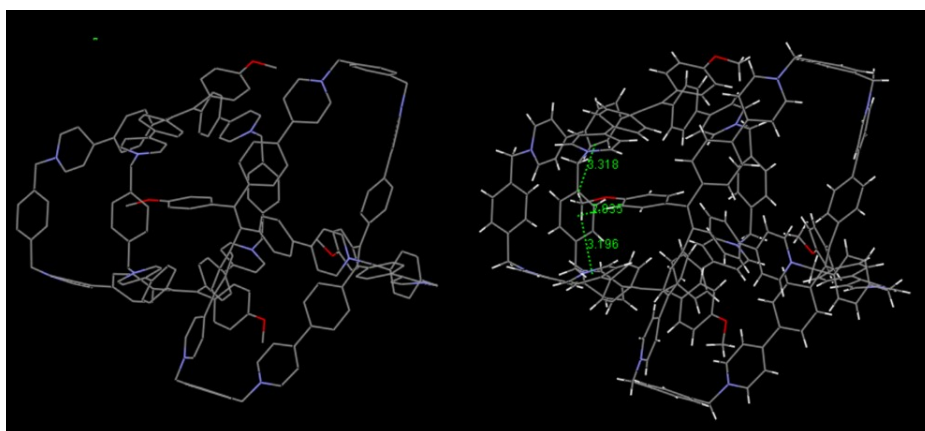


Figure S15. The X-ray crystal structure of cage dimer stabilized by C-H... π interactions. Color code: N, blue; C, gray; H, white; O, red.

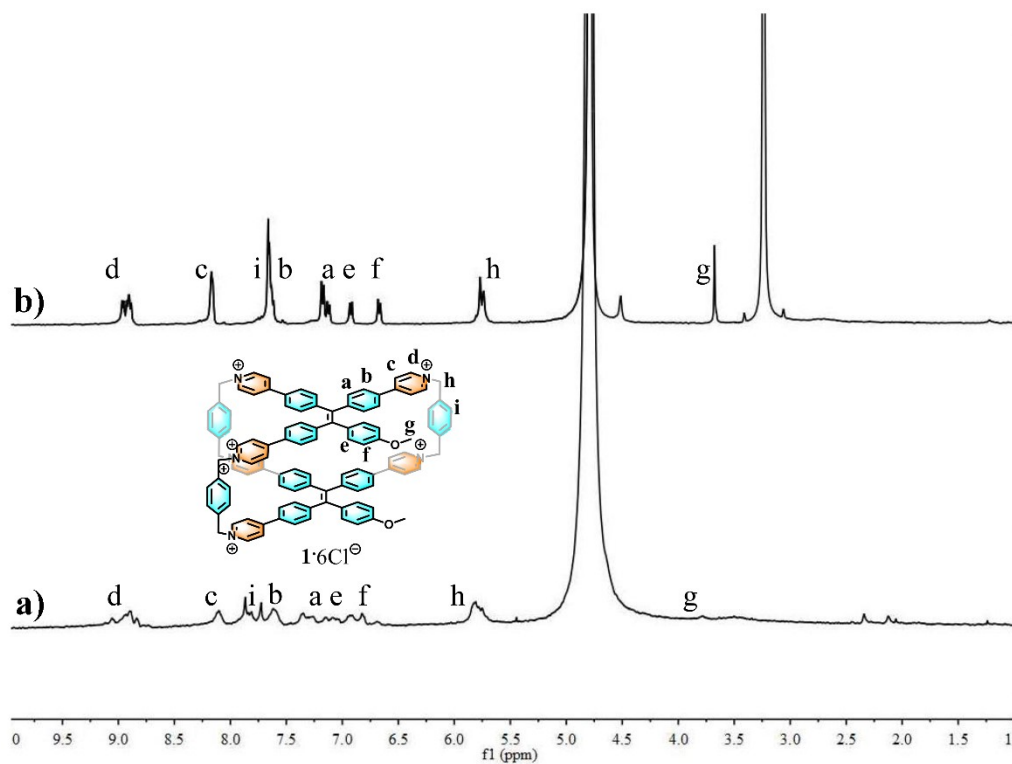


Figure S16. Solvent-dependent ^1H NMR (298 K, 400 MHz) of $1\cdot 6\text{Cl}^-$ in (a) D_2O and (b) CD_3OD .

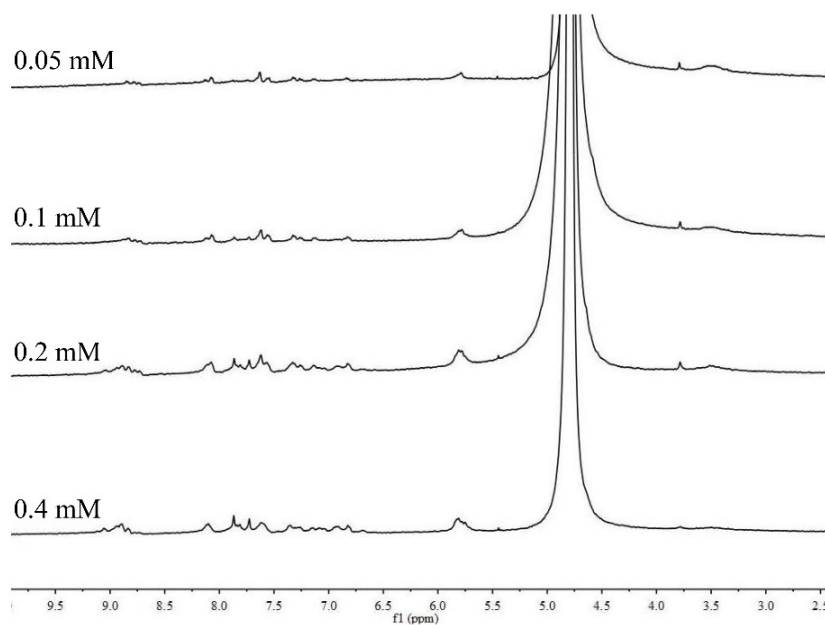
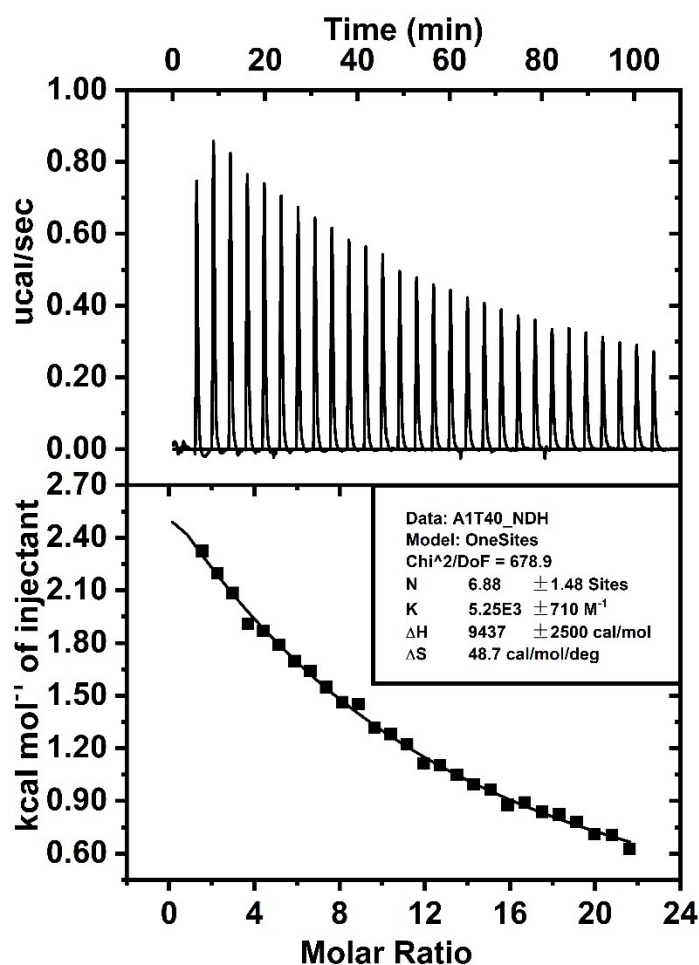


Figure S17. Concentration-variable (50 μM – 0.40 mM) ^1H NMR (298 K, 400 MHz, D_2O) of $1\cdot 6\text{Cl}^-$.



Thermodynamic parameters	1	2	3
K_a (10^3 M^{-1})	5.25 ± 0.71	5.60 ± 0.48	6.82 ± 0.38
ΔH (cal mol^{-1})	9437 ± 2500	13940 ± 3305	10150 ± 986.6
ΔS ($\text{cal mol}^{-1} \text{ deg}^{-1}$)	48.7	63.9	51.6

Figure S18. ITC titration curves of the dilution of $1 \cdot 6\text{Cl}^-$ at 298 K. In these titration experiments, the sequential injections of the dimer solution ($[1 \cdot 6\text{Cl}^-]_{\text{initial}} = 1.0 \text{ mM}$) into pure water solvent. The thermodynamic parameters for ITC experiments were repeated three times. The calculated average dimerization constant $K_{\text{dimerization}} = (5.89 \pm 0.52) \times 10^3 \text{ M}^{-1}$.

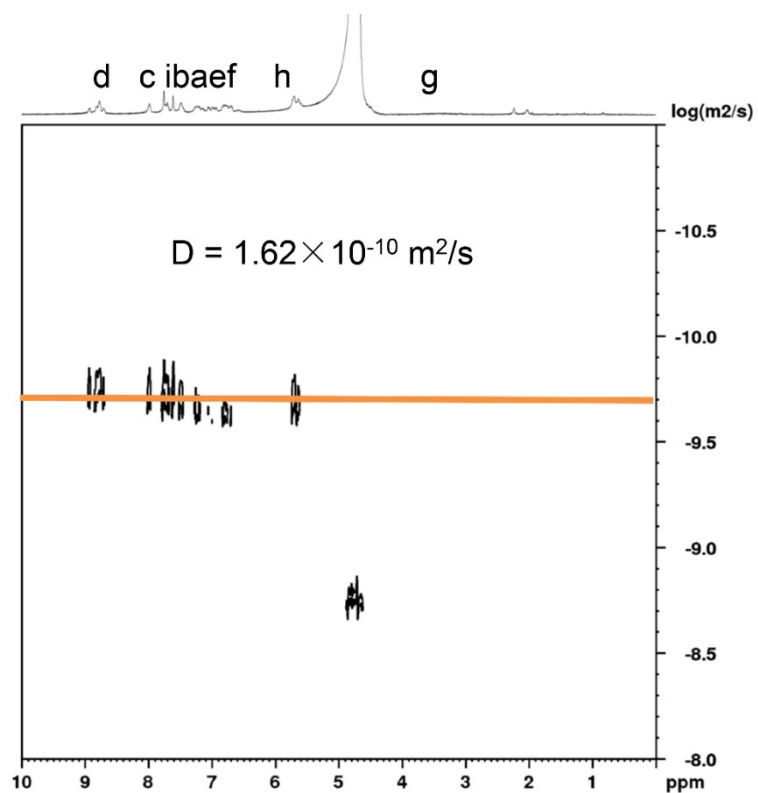


Figure S19. 2D DOSY spectrum (400 MHz, D₂O, RT) for **1**•6Cl⁻ (1.0 mM).

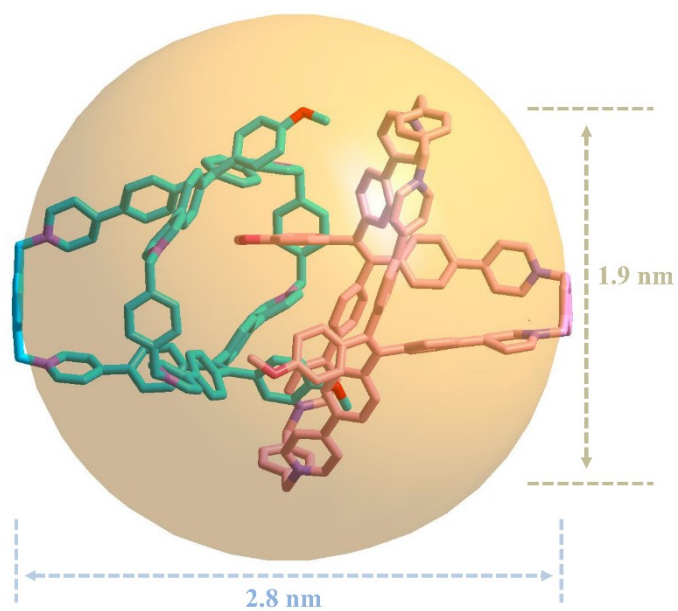


Figure S20. The sizes of dimer (**1**)₂.

Host-guest chemistry between $1\cdot6\text{PF}_6^-$ and PAHs

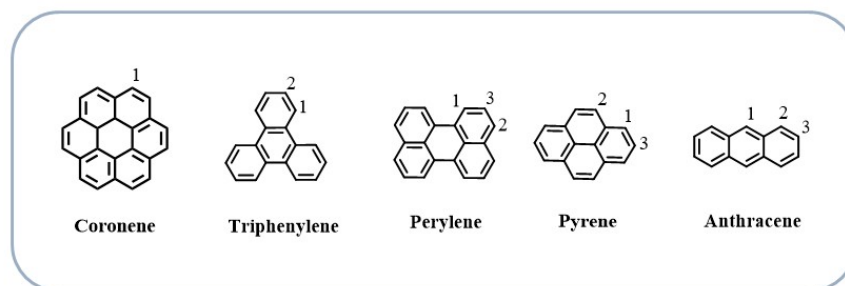


Figure S21. The chemical structures of PAHs.

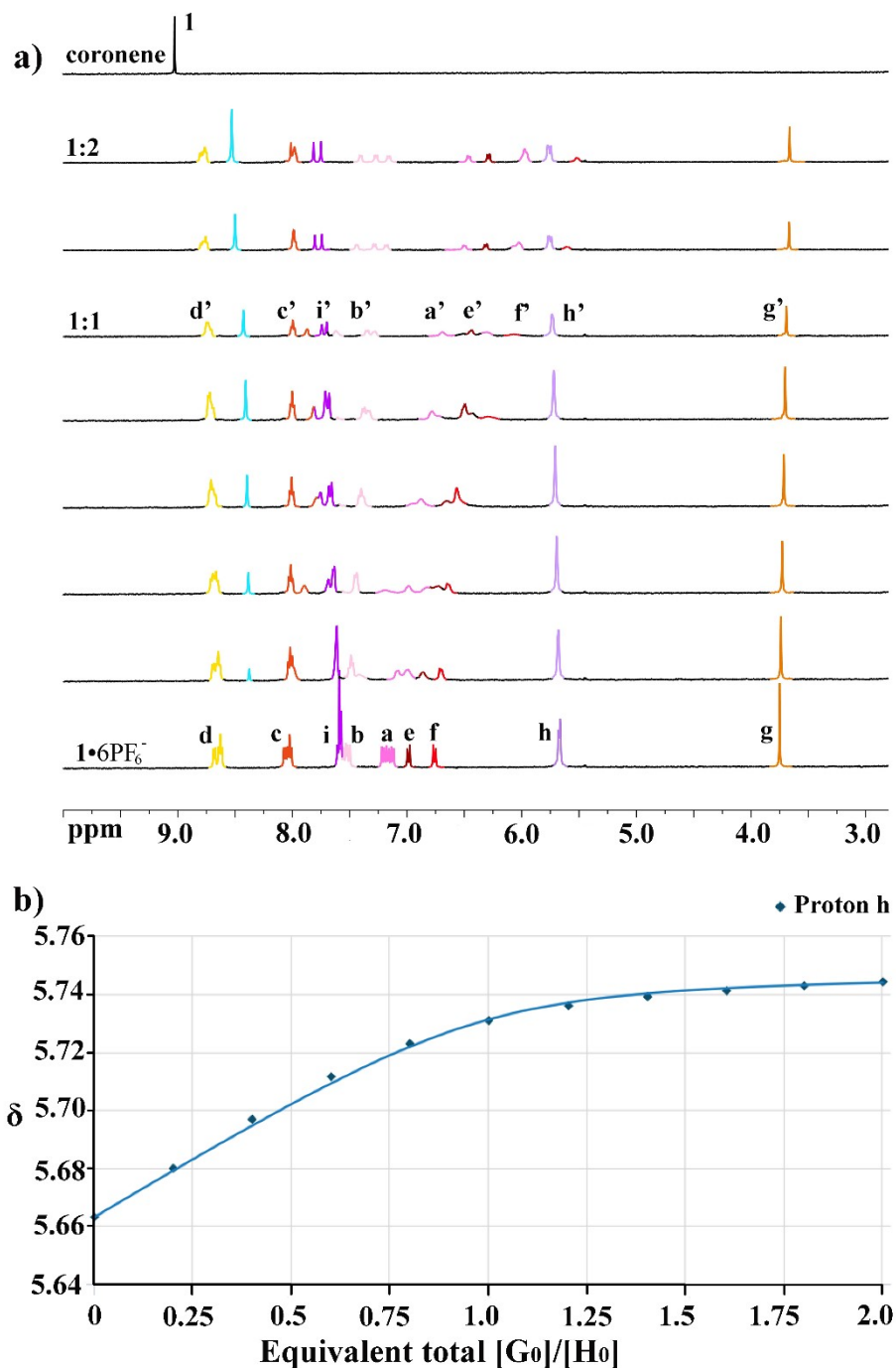


Figure S22. (a) ¹H NMR titration (400 MHz, 298 K, CD₃CN) of **1**•6PF₆⁻ (0.40 mM) with coronene (0 – 2.0 equiv). (b) Chemical shift changes plot of **1**•6PF₆⁻ (0.40 mM) titrated with coronene.

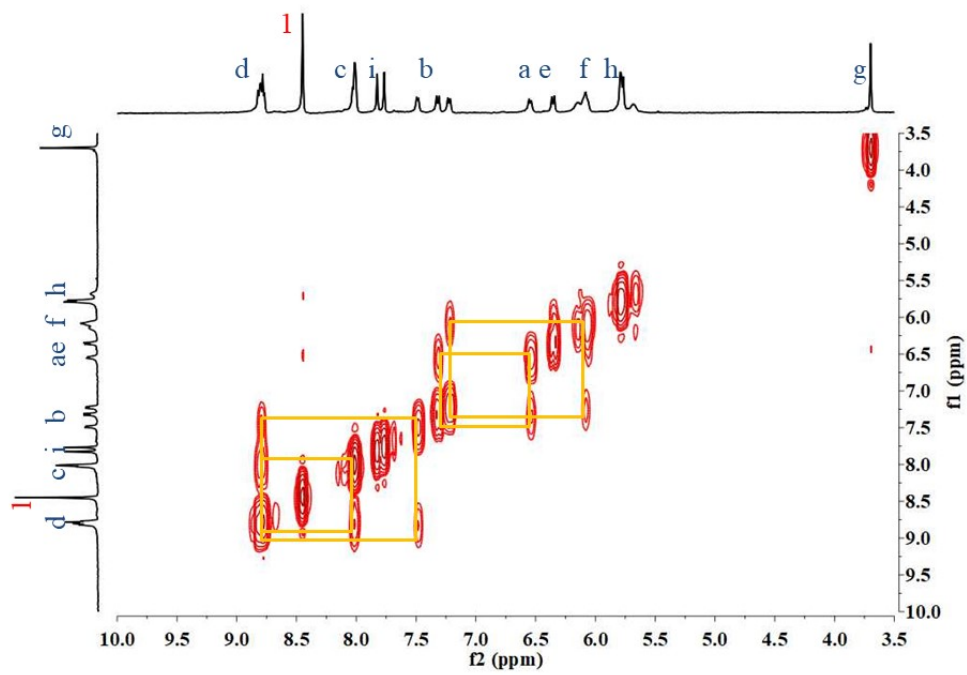


Figure S23. COSY ^1H NMR spectrum recorded (400 MHz, CD_3CN , RT) for $1 \cdot 6\text{PF}_6^-$ coronene.

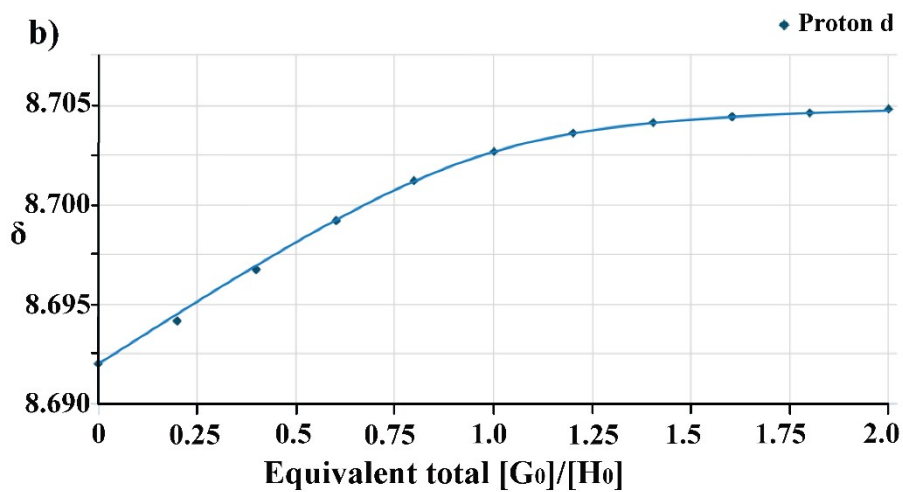
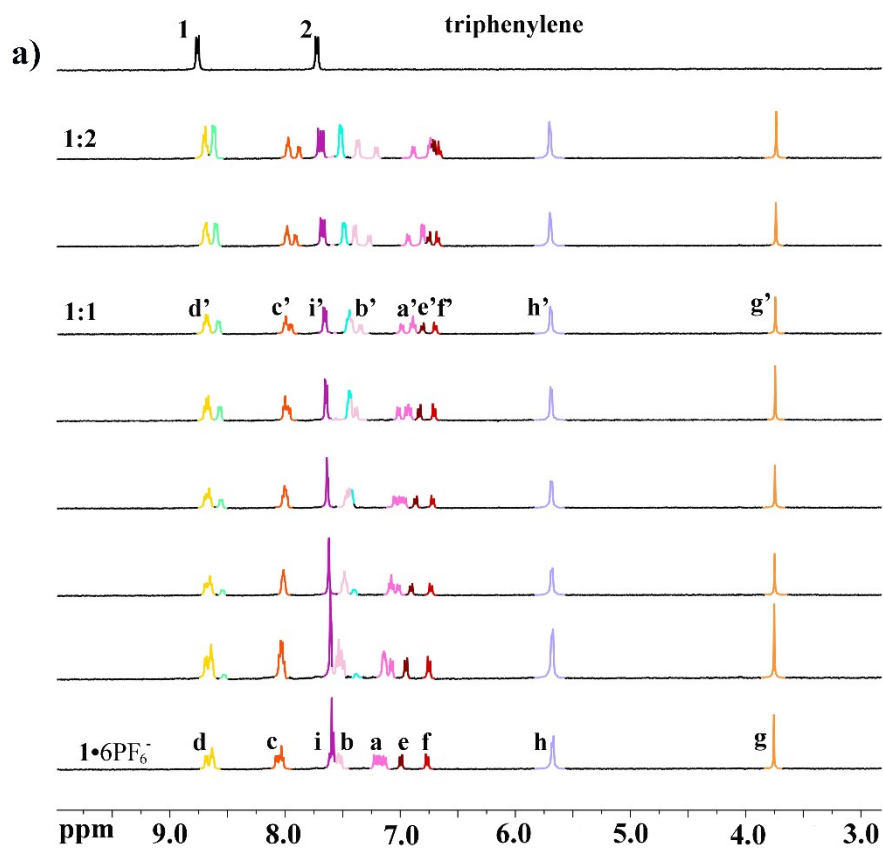


Figure S24. (a) 1H NMR titration (400 MHz, 298 K, CD_3CN) of $1 \cdot 6PF_6^-$ (0.40 mM) with triphenylene (0 – 2.0 equiv). (b) Chemical shift changes plot of $1 \cdot 6PF_6^-$ (0.40 mM) titrated with triphenylene.

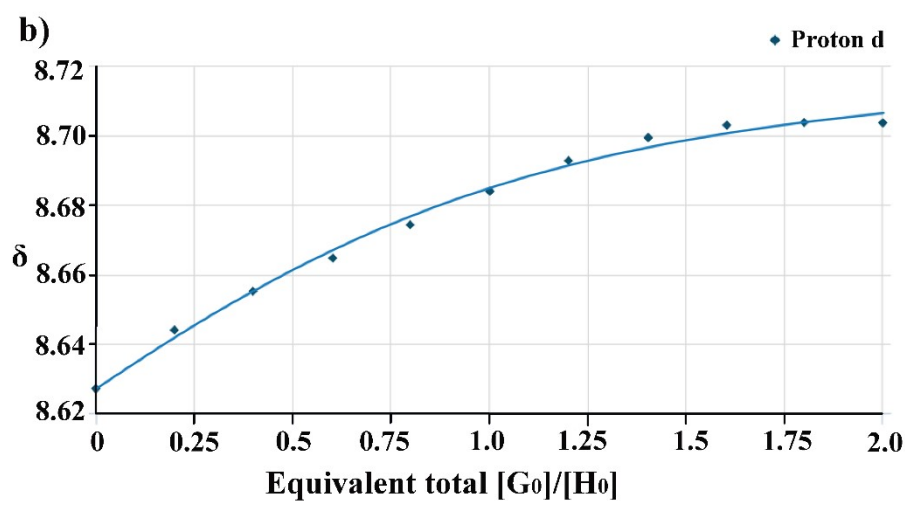
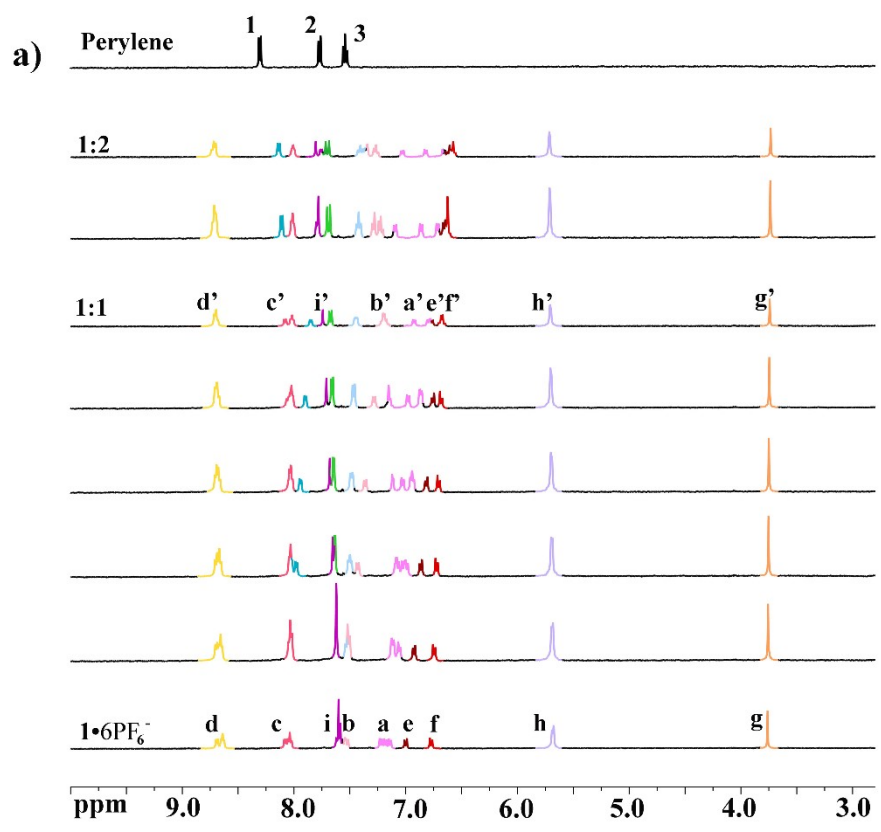


Figure S25. (a) ¹H NMR titration (400 MHz, 298 K, CD₃CN) of **1•6PF₆⁻** (0.40 mM) with perylene (0 – 2.0 equiv). (b) Chemical shift changes plot of **1•6PF₆⁻** (0.40 mM) titrated with perylene.

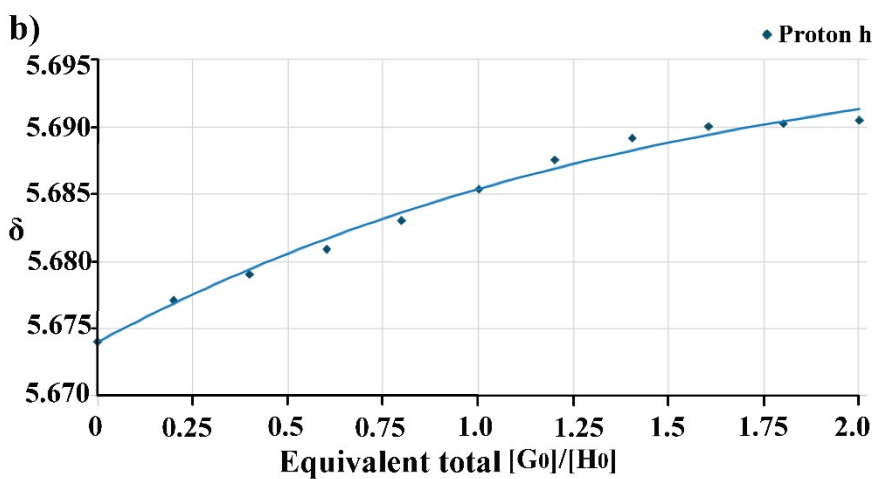
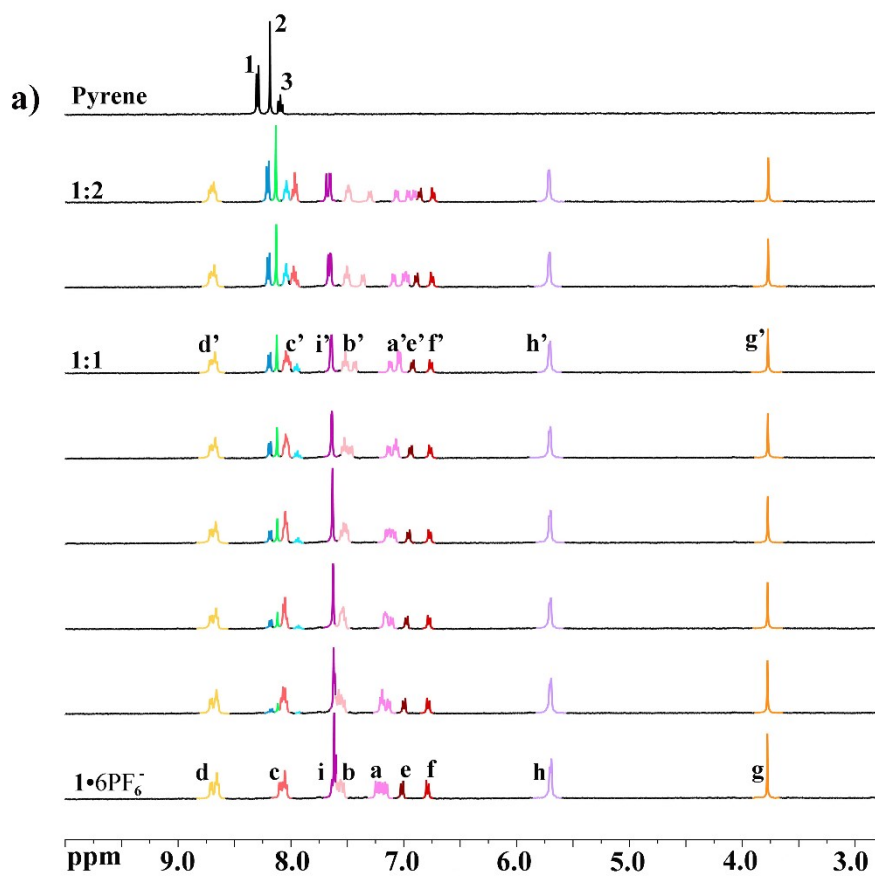


Figure S26. (a) ^1H NMR titration (400 MHz, 298 K, CD_3CN) of $1\cdot 6\text{PF}_6^-$ (0.40 mM) with pyrene (0 – 2.0 equiv). (b) Chemical shift changes plot of $1\cdot 6\text{PF}_6^-$ (0.40 mM) titrated with pyrene.

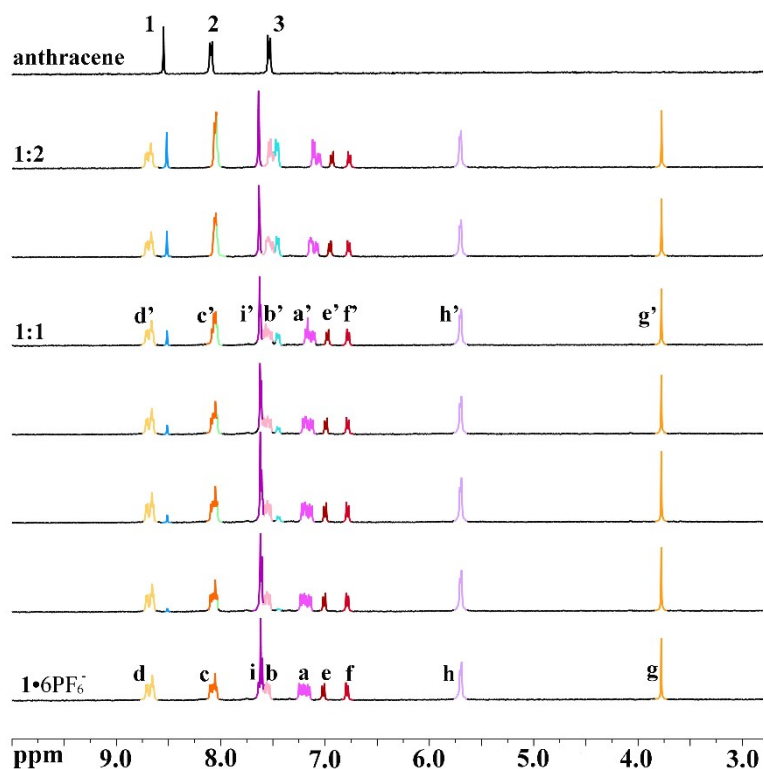


Figure S27. ^1H NMR titration (400 MHz, 298 K, CD_3CN) of $1\cdot 6\text{PF}_6^-$ (0.40 mM) with anthracene (0 – 2.0 equiv).

Table S2. The binding constants of H-G complex calculated by NMR.²

H-G complex	K_a (M^{-1})
$1\cdot 6\text{PF}_6^- \rightleftharpoons \text{coronene}$	$(2.36 \pm 0.08) \times 10^3$
$1\cdot 6\text{PF}_6^- \rightleftharpoons \text{triphenylene}$	$(2.05 \pm 0.01) \times 10^3$
$1\cdot 6\text{PF}_6^- \rightleftharpoons \text{perylene}$	$(7.07 \pm 0.72) \times 10^2$
$1\cdot 6\text{PF}_6^- \rightleftharpoons \text{pyrene}$	$(6.06 \pm 0.16) \times 10^2$

(The binding constant of anthracene was not obtained because of the weak host-guest interaction.)

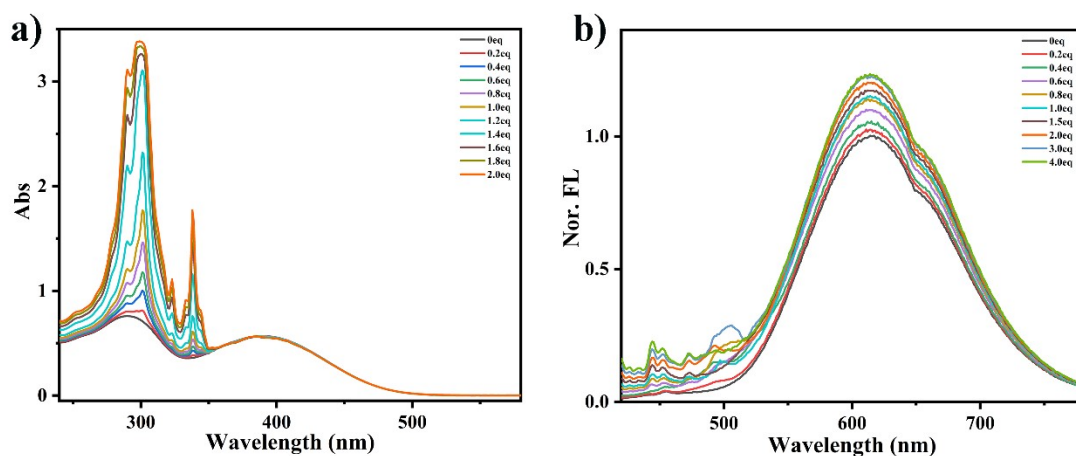


Figure S28. (a) UV-vis absorption and (b) fluorescence spectra of $1\cdot 6PF_6^-$ ($10\ \mu M$) in CH_3CN upon addition of coronene. $\lambda_{ex} = 400\ nm$, Ex/Em slit = $4\ nm$.

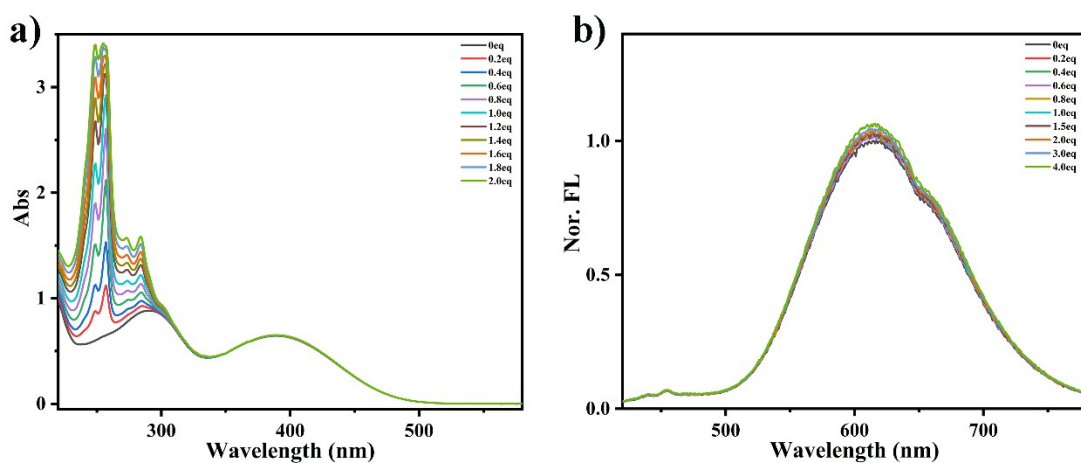


Figure S29. (a) UV-vis absorption and (b) fluorescence spectra of $1\cdot 6PF_6^-$ ($10\ \mu M$) in CH_3CN upon addition of triphenylene. $\lambda_{ex} = 400\ nm$, Ex/Em slit = $4\ nm$.

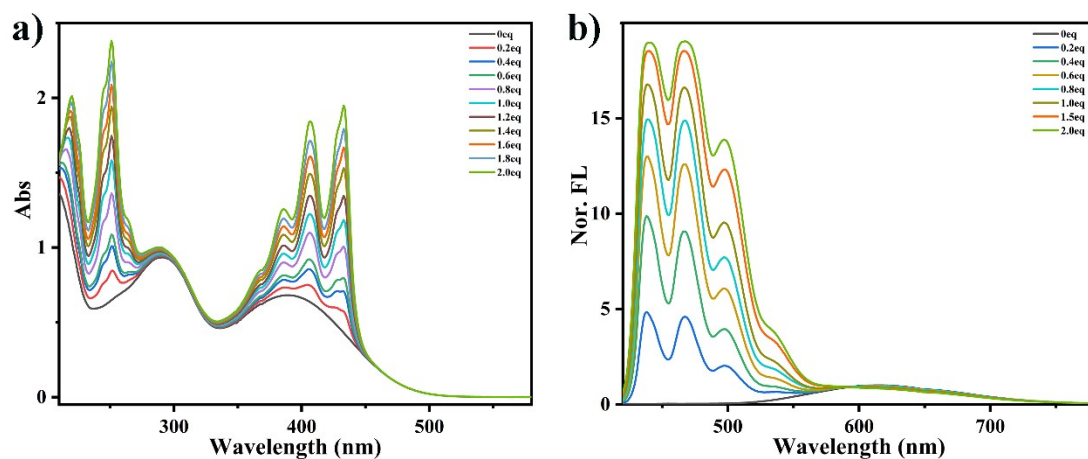


Figure S30. (a) UV-vis absorption and (b) fluorescence spectra of $1\cdot 6PF_6^-$ ($10\ \mu M$) in CH_3CN upon addition of perylene. $\lambda_{ex} = 400\ nm$, Ex/Em slit = 4 nm.

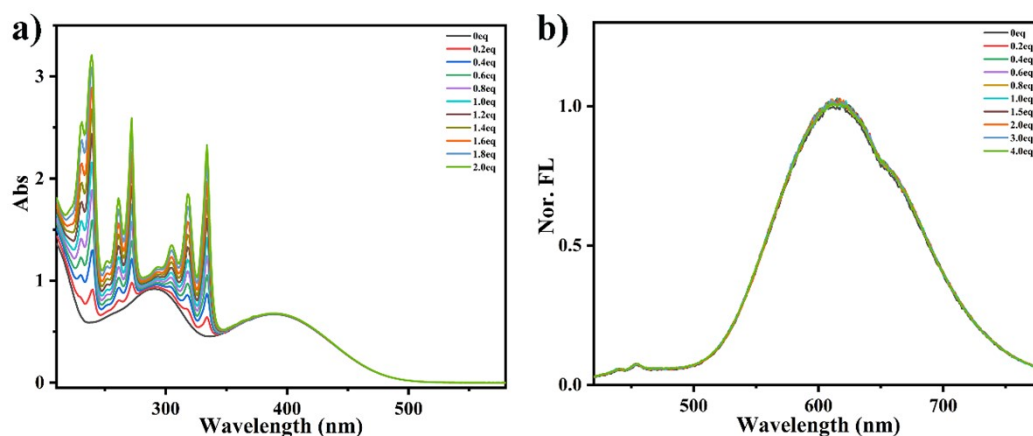


Figure S31. (a) UV-vis absorption and (b) fluorescence spectra of $1\cdot 6PF_6^-$ ($10\ \mu M$) in CH_3CN upon addition of pyrene. $\lambda_{ex} = 400\ nm$, Ex/Em slit = 4 nm.

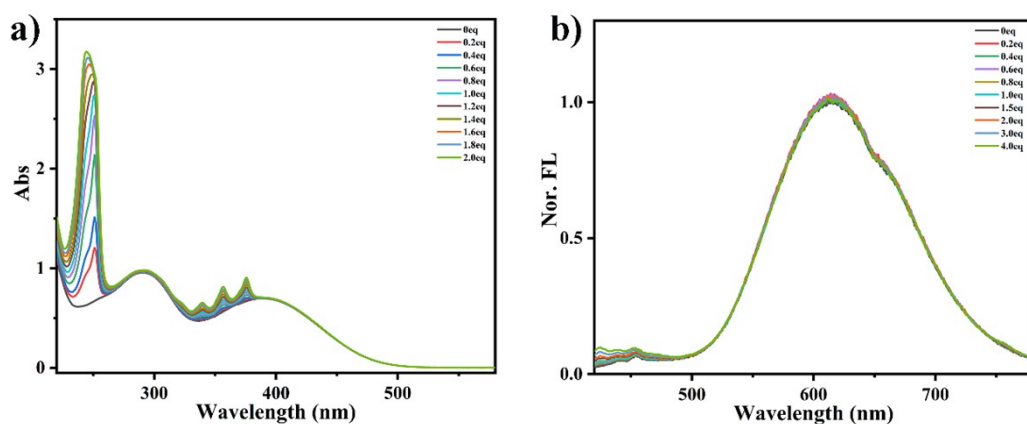


Figure S32. (a) UV-vis absorption and (b) fluorescence spectra of $1\cdot 6PF_6^-$ ($10\ \mu M$) in CH_3CN upon addition of anthracene. $\lambda_{ex} = 400\ nm$, Ex/Em slit = 4 nm.

X-ray Structure determination of $1 \cdot 6PF_6^- \supset$ coronene.

The crystal of $1 \cdot 6PF_6^- \supset$ coronene: $1 \cdot 6PF_6^-$ (0.57 mg, 0.2 mmol) and coronene (0.12 mg, 0.4 mmol) were dissolved in MeCN (0.5 mL) and the solution was passed through a 0.45- μ m filter into a 10 mL tube, which was placed inside a 500 mL wild-mouth bottle containing isopropyl ether (50 mL). The bottle was capped, after slow evaporation of isopropyl ether at room temperature into the MeCN solution for 3 days, and orange single crystals of $1 \cdot 6PF_6^- \supset$ coronene were obtained.

Table S3. Crystal data and structure refinement for $1 \cdot 6PF_6^- \supset$ coronene.

Chemical formula	$C_{132}H_{98}F_{36}N_6O_2P_6$
M_r	2669.98
Temperature	293(2) K
Wavelength	1.34139 Å
Crystal system, Space group	Orthorhombic, $Pna2_1$
a, b, c (Å)	48.4768(18), 17.0639(7), 16.7750(7)
α, β, γ (°)	90, 90, 90
V (Å ³)	13876.3(10)
Z	4
Density (calculated)	1.416 Mg/m ³
Absorption coefficient	1.067 mm ⁻¹
F(000)	6064
Crystal size(mm ³)	0.24 x 0.22 x 0.2
Theta range for data collection	2.755 to 52.981°
Index ranges	$-57 \leq h \leq 57, -14 \leq k \leq 20, -14 \leq l \leq 19$
Reflections collected	147092
Independent reflections	21996 [R(int) = 0.0460]
Completeness to theta = 25.242°	99.6 %
Absorption correction	Semi-empirical from equivalents

Max. and min. transmission	0.7508 and 0.6157
Refinement method	Full-matrix least-squares on F ²
Data / restraints / parameters	21996 / 3697 / 1514
Goodness-of-fit on F ²	1.073
Final R indices [$I > 2\sigma(I)$]	R1 = 0.0910, wR2 = 0.1862
R indices (all data)	R1 = 0.0974, wR2 = 0.1891
Extinction coefficient	n/a
Largest diff. peak and hole	0.742 and -0.584 e.Å ⁻³

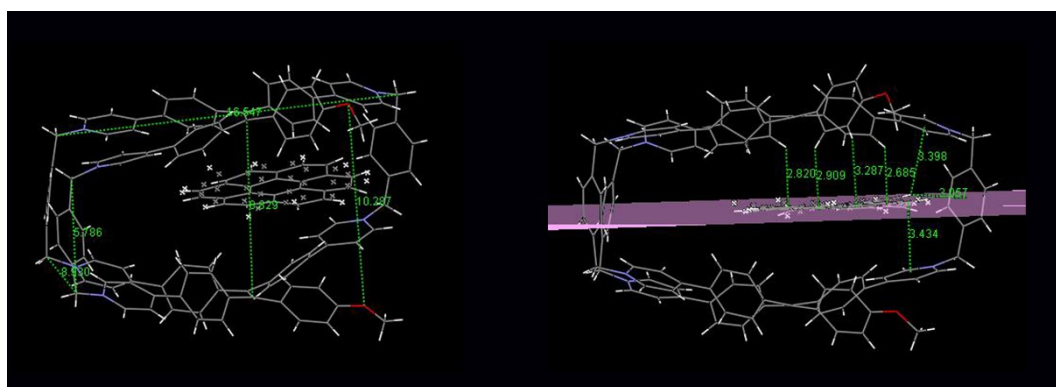


Figure S33. The X-ray structures of **1•6PF₆⁻⊃coronene** and the C-H•••π interaction. Color code: N, blue; C, gray; H, white; O, red.

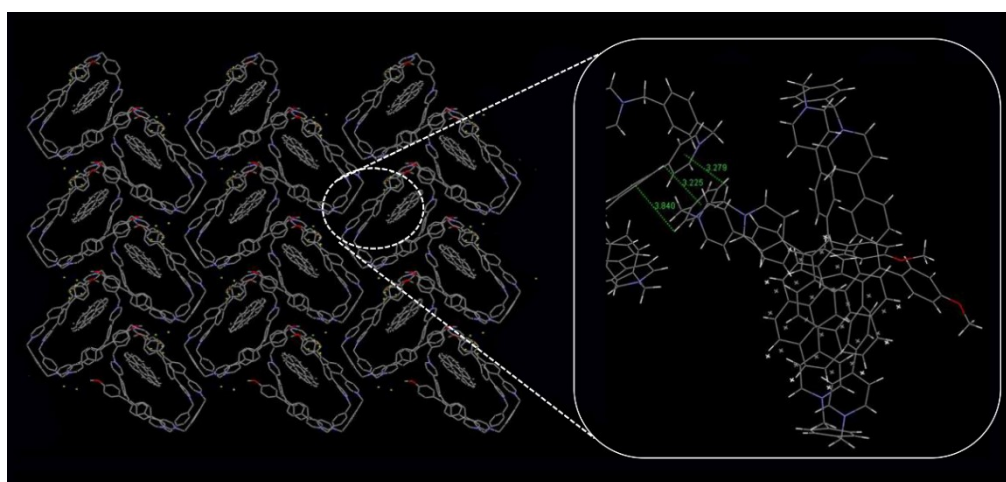


Figure S34. the stack packing of the host-guest complexes from b axis results in a 2D-layered structure and the C-H•••π interaction. Color code: N, blue; C, gray; H, white; O, red.

Host-guest chemistry between $\mathbf{1}\cdot\mathbf{6Cl}^-$ and dinucleotide molecules.

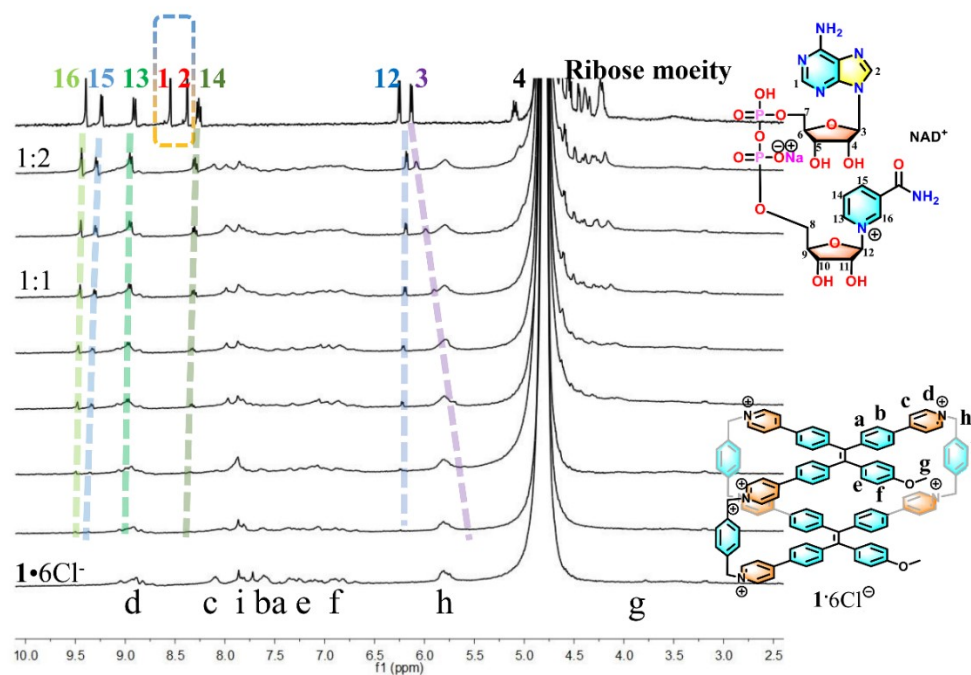


Figure S35. ^1H NMR titration (400 MHz, 298 K, D_2O) of $\mathbf{1}\cdot\mathbf{6Cl}^-$ (0.40 mM) with NAD^+ (0 – 2.0 equiv).

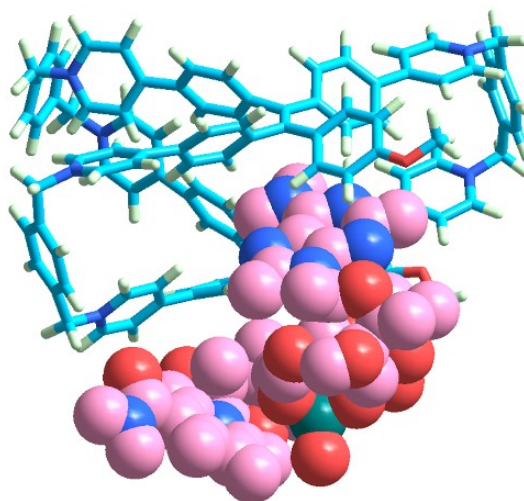


Figure S36. DFT calculation for the binding model of $\mathbf{1}\cdot\mathbf{6Cl}^- \supset \text{NAD}^+$. Color code: N, blue; C, light blue/pink; H, white; O, red; P, dark green. The structures were optimized using the gfn2-xtb method in Grimme's xtb softwareⁱ (version 6.4.1).³ The analytical linearized Poisson-Boltzmann (ALPB) model was used to account for the solvation effect of water.

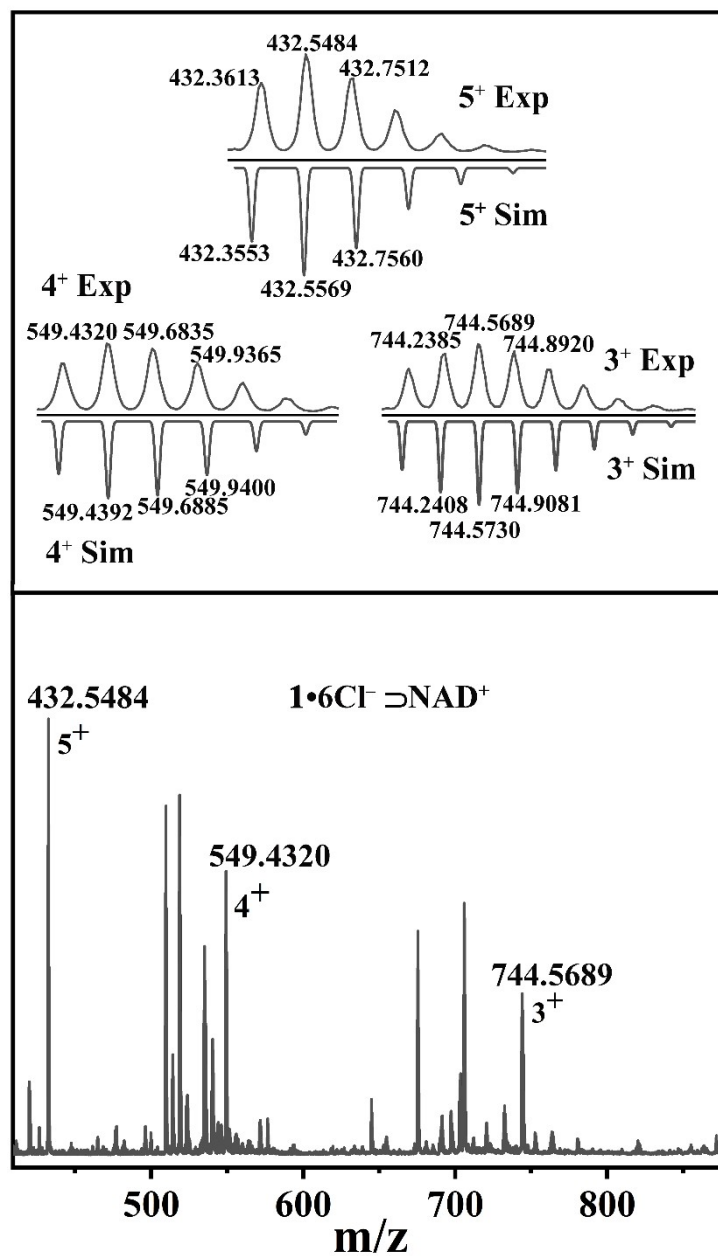


Figure S37. Experimental and calculated electrospray ionization mass spectra of **1•6Cl⁻ ⊃ NAD⁺**.

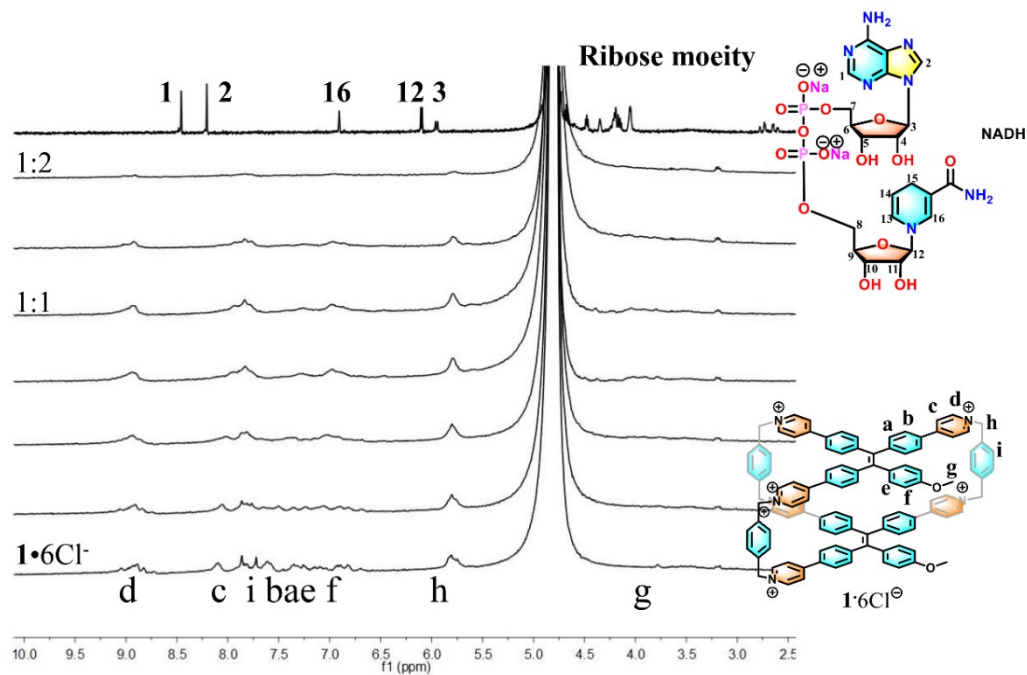


Figure S38. ^1H NMR titration (400 MHz, 298 K, D_2O) of $1\cdot 6\text{Cl}^-$ (0.40 mM) with NADH (0 – 2.0 equiv).

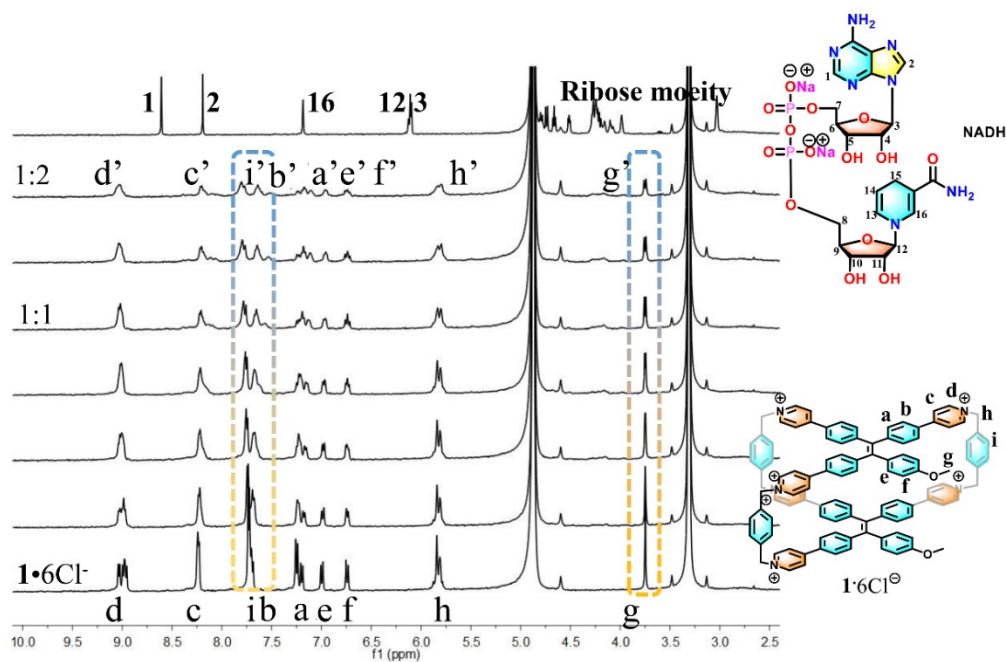


Figure S39. ^1H NMR titration (400 MHz, 298 K, CD_3OD) of $1\cdot 6\text{Cl}^-$ (0.40 mM) with NADH (0 – 2.0 equiv).

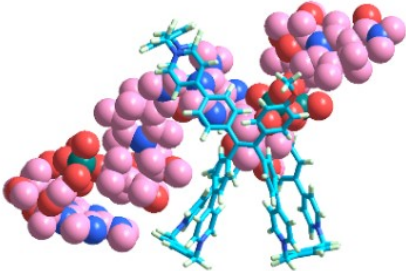
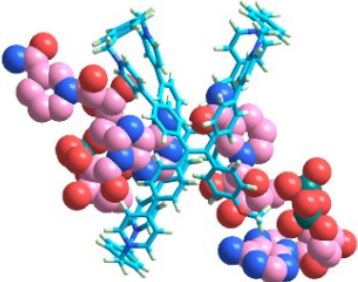
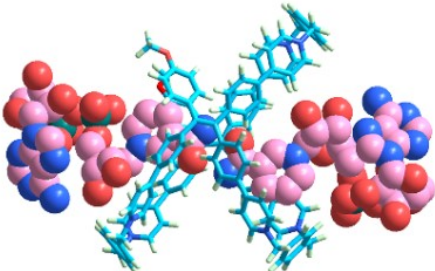
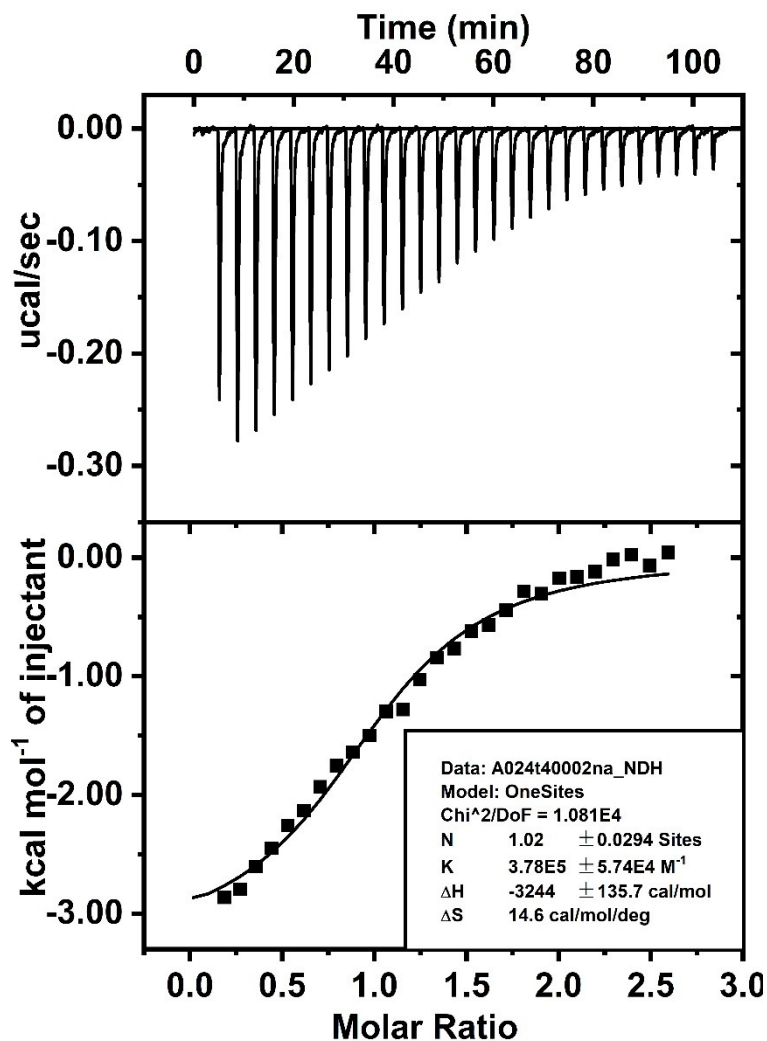
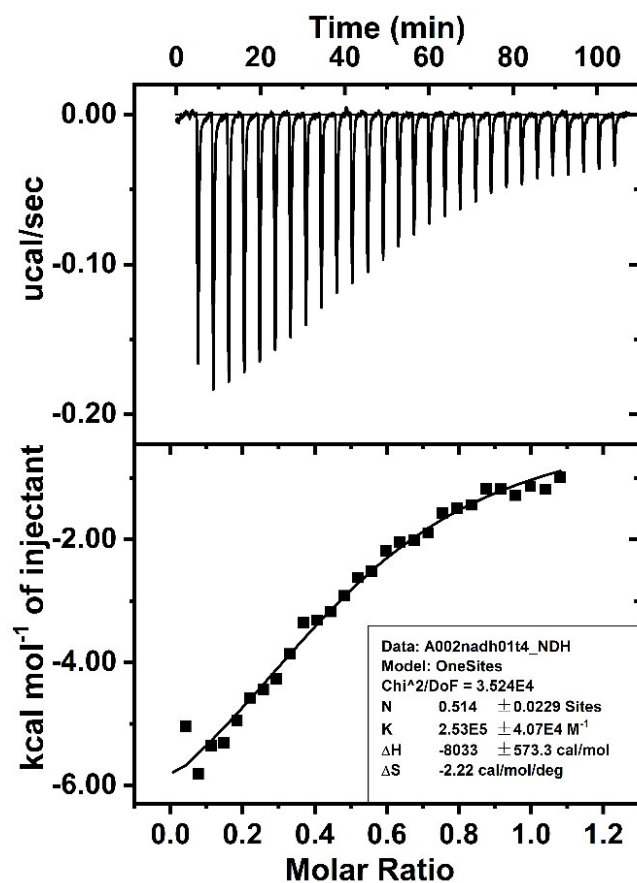
	Binding models	ΔE (Kcal/mol)
I		36.10
II		9.29
III		0

Figure S40. DFT calculations for three theoretically possible binding models of $\mathbf{1} \cdot 6\text{Cl}^- \rightleftharpoons (\text{NADH})_2$. DFT calculations support that III binding model is the most stable one among the three theoretically possible binding models. I model is the head-to-head complex; II model is the head-to-tail complex; III model is the tail-to-tail complex. Here, the tail is the nicotinamide unit; the head is the adenine unit. Color code: N, blue; C, light blue/pink; H, white; O, red; P, dark green. The structures were optimized using the gfn2-xtb method in Grimme's xtb software (version 6.4.1).³ The analytical linearized Poisson-Boltzmann (ALPB) model was used to account for the solvation effect of water.



Thermodynamic parameters	1	2	3
K_a (10^5 M^{-1})	3.78 ± 0.57	3.34 ± 0.83	3.30 ± 0.76
ΔH (cal mol^{-1})	-3244 ± 135.7	-3722 ± 131.9	-3414 ± 106.4
ΔS ($\text{cal mol}^{-1} \text{ deg}^{-1}$)	14.6	13.7	14.7

Figure S41. ITC data for the titration of NAD^+ (20 μM) in the cell with a solution of $1\cdot 6\text{Cl}^-$ (0.2 mM) in the syringe in water at 298K. The thermodynamic parameters for ITC experiments were repeated three times.



Thermodynamic parameters	1	2	3
K_a (10^5 M^{-1})	2.53 ± 0.41	2.35 ± 0.48	1.99 ± 0.39
ΔH (cal mol^{-1})	-8033 ± 573.3	-6497 ± 774.9	-8887 ± 763.8
ΔS ($\text{cal mol}^{-1} \text{ deg}^{-1}$)	-2.22	2.78	-5.56

Figure S42. ITC data for the titration of NADH (20 μM) in the cell with a solution of $\mathbf{1} \cdot \text{6Cl}^-$ (0.24 mM) in the syringe in water at 298 K. The thermodynamic parameters for ITC experiments were repeated three times.

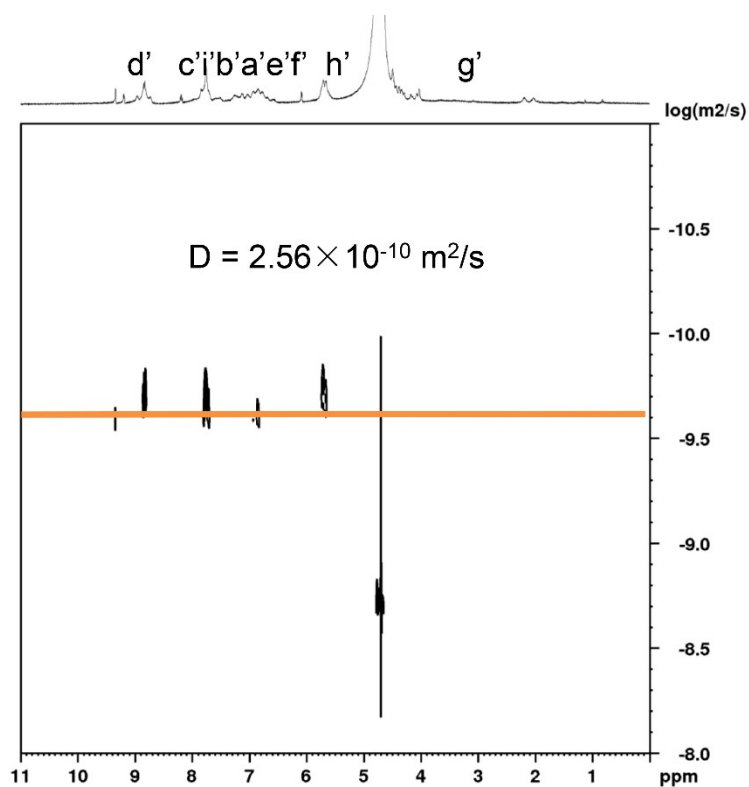


Figure S43. 2D DOSY spectrum (400 MHz, D_2O , RT) for $1 \cdot 6\text{Cl}^- \supset \text{NAD}^+$ (1.0 mM).

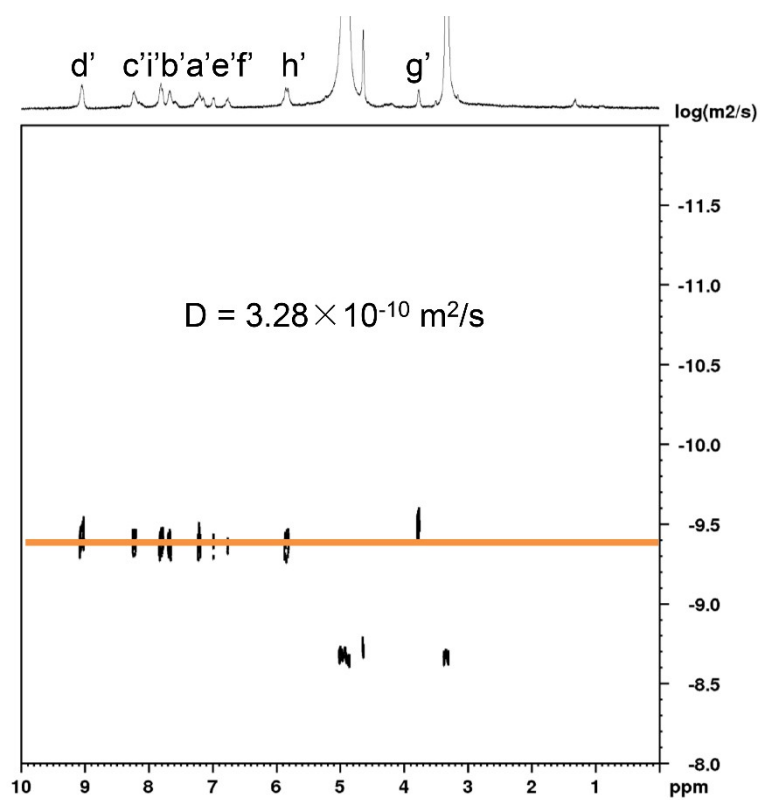


Figure S44. 2D DOSY spectrum (400 MHz, CD_3OD , RT) for $1 \cdot 6\text{Cl}^- \supset (\text{NADH})_2$ (0.6 mM).

Reference

1. S.-X. Nie, H. Guo, T.-Y. Huang, Y.-F. Ao, D.-X. Wang and Q. Q. Wang. *Nat. Commun.*, 2020, **11**, 6257.
 2. (a) P. Thordarson, *Chem. Soc. Rev.*, 2011, **40**, 1305-1323; (b) D. Brynn Hibbert, Pall Thordarson, *Chem. Commun.*, 2016, **52**, 12792-12805.
 3. C. Bannwarth, E. Caldeweyher, S. Ehlert, A. Hansen, P. Pracht, J. Seibert, S. Spicher, S. Grimme, *WIREs Comput. Mol. Sci.*, 2020, **11**, e01493.
-